ASSESSMENT OF CLIMATE CHANGE IMPACT ON RIVER FLOW REGIME AT MALAGARASI CATCHMENT-TANZANIA

A DISSERTATION REPORT

Submitted in partial fulfillment of the

the requirement for the award of the degree

of

MASTER OF TECHNOLOGY

in

HYDROLOGY

By

RESPICIUS SPERATUS

Reg No 17537009

Under the guidance of

Dr. D.S Arya

DEPARTMENT OF HYDROLOGY

INDIAN INSTITUTE OF TECHNOLOGY ROORKEE

ROORKEE-247667 (INDIA)

CANDIDATE'S DECLARATION

I hereby certify that this dissertation report entitled **"ASSESSMENT OF CLIMATE CHANGE IMPACTS ON RIVER FLOW REGIME AT MALAGARASI CATCHMENT-TANZANIA"** in partial fulfillment for the award of the **Degree of Masters of Technology in Hydrology, submitted** in the department of Hydrology of Indian Institute of Technology Roorkee, is an authentic record of my work carried out during the period of July 2018 to May 2019 under guidance of Dr. D.S ARYA, a professor , Department of Hydrology, Indian Institute of Technology, Roorkee.

The matter embodied in this work has not been submitted by me for the award of any other degree.

Date: ……..

Place: Roorkee

……

(Respicius Speratus)

Enrollment No-17537009

CERTIFICATE

This is to certify that the above statement made by the candidate is correct to the best of knowledge and belief

……..

(D.S Arya)

Professor

Department of Hydrology, IIT Roorkee

Roorkee- 247667.

India

ACKNOWLEDGMENT

I would like to express my significant feeling of most profound appreciation to Almighty God who gave me quality, wellbeing, and my understanding ability to attempt this task, my guide and help Prof. Dr. D.S Arya, for his important rules, which prompted my prosperity, compassion, and co-task. I express my gratitude to the Indian Technical and Economic Cooperation Program (ITEC) for giving monetary help, vital offices, and sources amid the whole time of my investigation.

Especially again my extraordinary thanks are coordinated to Dr. N.K Goel, Dr. Himanshu Joshi, Dr. M.K Manoj and Dr. M. Perumal who readily used their time bestowing information to the extent venture concern.

Finally, I stretch out my thankfulness to all Hydrology Department Staffs, who likewise among themselves contributed a lot to my learning condition at IIT Roorkee.

Special thanks ought to go to my family, my wife Beatrice Alexander, my son Renatus Respicius and my little girl Precious Respicius, my sisters Evelina Speratus, Conchesta Speratus and Angelica Speratus and sibling Novatius Speratus and the majority of my colleagues in addition to my granddad Cyprian Rwakatare for their exceptional consolation through the whole time of my investigations.

IIT Roorkee …….

Date: …….. Respicius Speratus

ABSTRACT

In this specific investigation to evaluate, the climate change on river flow regime a semi-distributed conceptional model was used for simulating rainfall-runoff in Malagarasi catchment-lake Tanganyika basin, Tanzania. The IPCC-DDC website was used to extract the future prediction of the climate signal of temperature and rainfall from the multi-model of the Global Climate Model (GCM) of the CMIP5. The two global climate scenarios of RCP4.5 and RCP8.5 were used to project future expectations. However, HBV Light model then forced with the ensemble mean of the downscaled daily temperature and rainfall from SDSM model to simulate the daily future runoff at the outlet of the Malagarasi catchment for near future (2020-2045), middle future (2046-2075), and late future skyline (2076-2099) of the 21st century.

The downscaled rainfall have shown no change in total annual rainfall but the declining trend from January to April (during the wet season), and increasing trend of October to December and with a marginal change in May to September. Man-Kendall's test showed that the forecasted temperature depicts declining trend in most GCMs, insignificant at 5% significant level.

The HBV (Hydrologiska Byrans Vattenbalansavdelning) light model was calibrated and validated with past rainfall, temperature and discharge data of 5 to 10 years. The satisfactory results were obtained and producing NSE between 0.85 to 0.87 for all cases. The calibration period was from 2000 to 2010 with a period of ten years and validation was from 2011 to 2015, a period of five years. Also, the coefficient of determination R^2 was checked and the results were ranging between 0.86 to 0.88 for both cases. Also at the outflow of the catchment, it is noted that there is a decrease of discharge which tends to decrease yearly. The magnitude of the trend for historical data was tested using Thiel-Sen's Slope median estimator, which indicated that most of the trend is insignificant at 5% significant level.

All scenarios of RCP4.5 and RCP8.5 from each selected GCM of CSM1.1, MIROC, BNU-ESM, and CanESM2 have shown the declining trend of river flows for the period of January to April ranging from 5.6% to 27.3% when compared with the observed period. The rest of the months shown a marginal increase in river flows ranging from 5.1% to 9.8%. The mean annual river flow depicts the declining trend running from 4.39% to 19.17% expect CSM1.1 GCM, which showed an increasing trend ranging from 9.86% to 18.47%. Furthermore, the maximum and minimum

river flows during the high and low season have depicted a declining trend of 9.8% to 27.8% and 1.76% to 21.35% respectively when compared with the observed period.

LIST OF FIGURES

LIST OF TABLES

TABLE OF CONTENTS

LIST OF ABBREVIATION AND SYMBOLS

a.m.s.l	Above Mean Sea Level
BETA	The parameter that determines the relative contribution to runoff from rain or snowmelt (-)
BCC	Beijing Climate Center
BNU	Beijing Normal University
CCCma	Canadian Centre for Climate Modelling and Analysis
CMIP	Coupled Model Intercomparison Project
CMIP3	Coupled Model Intercomparison Project Phase 3
CMIP4	Coupled Model Intercomparison Project Phase 4
CMIP5	Coupled Model Intercomparison Project Phase 5
DEM	Digital Elevation Model
DP	Daily Percentage
E	Evapotranspiration
ETo	Averaged Reference Evapotranspiration
ETp	Potential Evapotranspiration
FC	Field Capacity
GAP	Generic Algorithm and Powell Optimization
GCM	Global Climate Model
GIS	Geospatial information system
GUI	Graphical User Interphase
HBV	Hydrologiska Bryans Vattenbalansavdelning
HS	Hargreaves and Samani
IPCC	Intergovernmental Panel on Climate Change
Km^2	Square Kilometers
LAM	Limited-Area Model
LARS-WG	Long Ashton Research Station-Weather Generator
LTBWB	Lake Tanganyika Basin Water Board
LZ	Storage in the lower reservoir
ModB	Model-Base Bias Correction

NASA	National Aeronautics and Space Administration
NSE	Nash Sutcliffe efficiency
P	Precipitation
PBIAS	Percentage of Bias
PERC	Percolation
Q	Total Runoff
Q_0	Fast Runoff component
Q_1	Slow Runoff component
QM	Quantile Mapping
R^2	Coefficient of Determination
RCM	Regional Climate Model
REMO	REgional MOdel
SDSM	Statistical Down-Scaling Model
SM	Soil Moisture
SMEC	Snowy Mountains Engineering Corporation
SP	Snow cover
SWAT	Soil and Water Assessment Tool
Tmax	Maximum Temperature
Tmean	Average Temperature
Tmin	Minimum Temperature
UZ	Storage in an upper reservoir
WEAP	Water Evaluation and Planning System
WGs	Weather Generator
WRBWO	Wami Ruvu Basin Water Office

CHAPTER ONE: INTRODUCTION

1.1 Background

Climate change is the greatest challenge that the whole world is facing now in which its impacts have affected water resources, which later could become diverse and uncertain. According to Saqib et al, (2010), changes caused in extents of stream flows will be prone to increase tension among the regions living in downstream zones concerning decreased river flows in the dry season and high flows with coming about flood amid the wet season. Zhenya et al., (2018) has described such the adjustments in the river flows could prompt a genuine arrangement of negative effects on stream environment such as termination and invasion of extraordinary species.

Instabilities and alteration of river flow routine initiated by the environmental change has great negative impacts on sustainability and management of water resources, especially when maintaining environmental flow for the stream that is diversely affected. Fast growing of anthropogenic activities taking place around the globe will speed up negative impacts on water resources, river, streams, aquatic species, and ecosystem, which will bear extreme events like flooding, drought, the rise in temperature, sea saltwater intrusion, rise and fall of sea water levels and loss of biodiversity. In the IPCC (2007) fifth assessment report, it is have stated that rise of temperature and falling of rainfall pattern with increased frequency of extreme climate events such as flooding, drought, are expected future climate in the tropics.

Asfaw (2017) explained the current climate variability is now forced a critical test to water and vitality supply, water system plans, neediness decrease, and hydropower age just as causing regular assets exhaustion and common calamities. In this manner surveying, the effect of climate change on river flow variations in Malagarasi catchment are expected to have a significant implementation on water resources management plans, agriculture productivity, and hydropower production and with its operation.

Tanzania due to global climate change is experiencing seasons of erratic rainfall and drought. These changes in climate conditions have brought extreme weather condition such as temperature rise, shrinking of the ice sheet at Mount Kilimanjaro, reduction of snow cover that could lead to extreme events like floods and drought. Increase in the occurrence of these events could lead to

river environmental degradation and pollution. Rivers being the major source of energy (electricity) as well as a source of domestic water supply, industrial and irrigation, plans needed, better management and monitoring.

The IPCC (2013), the fifth assessment report has shown that it is expected during the dry period a significant decline of discharge in most of the rivers. More rapid population in most cities and towns and increased temperature will lead to a shortage of water in the middle of the 21st century. Also, the report has shown an increase of extreme events especially during dry and wet periods, whereas in the dry period it is expected to extend for more than a normal period and results in extreme low flows and in wet season more intense rainfall is expected within a short time resulting to flooding.

Impact assessment at basin/catchment scale of climate change using mean annual runoff play an important role when assessing water resources in context to climate change even though seems to be more simplistic. Employing hydrological modeling that considers other weather parameters like evapotranspiration and temperature try to make more realistic than before using only rainfall for runoff forecasting. Due to the advancement of forecasting models, uncertainties due to limited knowledge on atmospheric processes and its interaction which tend to bring vagueness when comes to project future climate. Hence, the effect of environmental change on hydrology has been addressed year to year but still interesting and challenging topic due to incomplete knowledge on land and atmosphere response with increased anthropogenic activities, greenhouse gas emission, and human activities.

Many researchers have shown that there will be a significant change in hydrological river basins responses due to change of rainfall pattern around the global and increased extreme events. As per IPCC (2013) fifth assessment report, precipitation is expected to increase at higher latitudes prompting expanded winter/spring overflow and flooding in certain regions.

Hardy et al., (2003), has expressed in his book, worldwide and provincial changes in precipitation and evaporation will build late spring, vanishing and diminishing in surface flow and soil dampness at the mid of the high latitudes expected in the mid future.

Climate change assessment needs more knowledge about the atmosphere since the Earth is undergoing changes unprecedented in human history. According to Kendal et al., (2005), the

increase of the concentration of greenhouse gases, depletion of stratospheric ozone and changing of the chemical composition of the atmosphere may reduce the ability to cleanse through oxidation which could lead to significant change. These global changes lead to an imbalance of climatic conditions under which life was sustained for a long time. The IPCC has shortlisted that also there is a need for policy-makers to involve specialist since adaptation must comply with policy and friendly to environment and people which must be stated well in governance state policies.

Tanzania is among the countries that are passing through erratic climate change consequences in south sub-Saharan countries. Climatic regime and variability are now experienced in many parts of the country in which some place is characterized by prolonged drought, the rise of temperature and flooding. In the central part of the country that comprise Tabora, Singida and Dodoma regions are adversely affected with drought during the dry period. Morogoro, Dar es Salaam and Coast region found eastern part of the country much affected with flooding during the wet season, example consecutive three years of flooding in 2016, 2017, and 2018 at Jangwani wetland in Dar es Salaam and Kilombero in Morogoro. In these regions, people were displaced to other place hosting them for some days during the event. Also, there is a one-time event in rest of the region even though not frequent which also risk the life of people and their properties example flooding in Bukoba town on 8 April 2017 where more than 100 inhabitants were affected.

Climate change uncertainty has induced more tension on residence who mostly depend largely on water resources available due to unprecedented occurrences. Assefa et al., (2012), has shown that there will be considerable consequences on fauna and flora because of environmental change that yet occurring in numerous gatherings of the nation. He also pointed out that due to existing signal and increased rainfall of more than 50% that will tend to double the runoff during the wet season, which could result in flooding. He suggested that if the climate goes like what predicted, there is a need to strengthen the infrastructure and an integrated approach towards water resources management and proper adaptive measure plans.

River flow alteration will affect aquatic organisms and human being since water available for supply, hydropower generation, irrigation, and navigation will not be adequate. In other stream and rivers, maintaining environmental flow for sustaining aquatic will be a great job.

Julie et al., (2010), pointed out the qualitative analyses of ecological consequences on flow alteration. The negative ecological consequences will accelerate the invasion of exotic; endanger species and disappearing of most of the species within the river and other water bodies.

The evaluation of environmental change impacts on hydrology has been tended to for quite a while. It has been constantly revised thanks to the improvement of climate model outputs regarding spatiotemporal resolution and projection capability. Most estimations depend essentially upon the coupling method between worldwide atmospheric General Circulation Models (GCMs), which are set up to simulate the past and current atmosphere and after that used to extend the future condition of the worldwide atmosphere with explicit ozone-harming substance emanation situations and hydrological models. Although climate models can be expected to project trends correctly, different climate models can give different outputs. In other words, the application of various climate model outputs often results in discrepancies in runoff simulations. Assessment of climate change impacts with multi-climate models has been exhibited as a cost-effective method to determine the scope of the project in the Coupled Model Inter-comparison Project (CMIP). Global Climate Model (GCM) is generally utilized devices to create projections of the future atmosphere IPCC, (2007) Because of their low spatial goals for hydrological application, their yield ought to be downscaled to higher spatial resolution.

Seasonal variation of river flow in some large river/lake basins was estimated in the most recent evaluation. The Fifth Assessment Report directed by the IPCC is a precedent, utilizing propelled atmosphere models created by prominent modeling associations around the globe (CMIP4). The report demonstrated that a huge decrease in the river flows is normal amid dry seasons. Expanding temperature and fast populace development in the vast majority of these basins will prompt extreme water deficiencies by the mid of this century. Other research shows that flood flow during wet periods is expected to increase in frequency under most climate change scenarios. Moreover, it is normal that hydrological reactions are disparate in each particular river basin because of the distinction between topography and weather patterns. Tanzania is one of the nations most influenced by climate change and the country has grown to consider it as a primary challenge in recent decades. With regard to adaptation techniques to environmental change, valuations of river flow variations at the catchment scale can furnish decision-makers and uncovered networks with basic information for the improved advancement of water resources management. This

examination displays a projection of runoff change in the Malagarasi river catchment as a contextual analysis. The precipitation prediction amid the time of 2020-2045, 2046-2075 and 2075-2099 under various climatic scenarios simulated by multi-atmosphere models are utilized as a contribution for a semi-distributed hydrological model to estimate flow varieties.

Modeling and simulation of system are highly stimulated and also sometimes are implemented for the river basin planning and management, for timely flood alert (early warning) and mapping areas with risk of flooding or flood risk zones, buffer zones of program of water budget especially for small water basins, according to regional and national regulations (Arish et al., 2010)

Tanzania like another country in African countries is affected much with climate change due to variability and unpredictability of climatic variables. Many rivers have changed from perennial to the non-perennial river and verse versa. Malagarasi catchment is among the catchment influenced much with environmental change on the grounds. The greater part of some streams in the northern part of the catchment has now dried up and in the focal part where wetland dominates likewise have changed to land. Expanded late spring, vanishing, expanded dry season frequencies, diminishing precipitation, diminishing lake levels in certain regions, change in wetland network; temperature routine is the dominating difficulties confronting the catchment.

Vice Presidents Office, (2013) have reported that climate change in the Tanzania coastal areas of the Indian Ocean basin is expected to exacerbate environmental and social problems which will intensify, affecting fishers, coastal residents resources users, recreation, infrastructure, and tourism development. Also have reported that there is an example of vulnerability in the region, which include the alarming scenario such as the rise of sea level of around 0.5 meters along Tanzania's 800 kilometers coastline, which is expected to inundate 247 square kilometers of area. Though quantitative projection was done based on rainfall patterns, the rise of sea level and tropical storms across the coastal, environmental protection still uncertain for adaptation and management.

Malagarasi catchment among the biggest and largest catchment that contains 33% of the absolute zone of Lake Tanganyika basin area. A catchment with multi-human activities includes

heterogeneous agriculture, fishing, brick making, wood charcoal burning, and other related social activities.

Kashaigili, (2010) has stated that the land cover land use has been depleting day to day due to improper use of land, poor management practice, deforestation, and change of climate variability. A noteworthy change in land use/cover for the period from 1984 to 2001 was also noticed. Also showed that there are decrease areas of woodland and wetlands vegetation cover of more than 1% per year. Natural issues like drying of stream and rivers, change in precipitation patterns, expanded soil disintegration and decreased harvest yield expected to be more prominent in the catchment. In most part of the catchment shown an early warning of some rivers and streams to dry up due to increased human activities along the banks of the rivers. Deforestation due to agriculture and charcoal burning have brought more tension on rainfall change pattern which causes the late start of agriculture season especially for farmer depending on rainfall. In most of the seasons, there is a delay of one to two months before rainfall starts, which needs proper management of land in order to sustain the climate.

1.2 Problem statement

The Malagarasi catchment is located western part of Tanzania, at an altitude of 773 to 1800 m and runoff from this catchment provides water for multi-sectoral purposes such as fishery, industry, agriculture and hydropower generation. Because of disturbing indications of a worldwide temperature alteration and environmental change, could later adjust the atmospheric conditions and hydrological responses of the catchment. Since the catchment is not developed in term of the flood control, reservoir, dam and water resources management plans, it is important to assess the runoff variation at the catchment scale in context to climate change scenarios. The use of hydrological modeling and simulation tools for climate change predictions during different climate change scenarios will help to understand the responses of the catchment.

1.3 Research Questions and Objectives

i. What is the effect of climate change on Malagarasi river flow regimes and in what way the catchment may be managed sustainably?

ii. Does the use of the HBV model give a good prediction for streamflows of the Malagarasi River?

1.4 Specific Objectives

i. Analysis of recent temperature, the river flows, and rainfall trends to understand the climate-induced changes in the catchment.
ii. Analysis of the future trend of rainfall and temperature using the SDSM statistical downscaling tool
iii. Predictions of future streamflow (runoff) under different climate change scenarios using HBV

1.5 Thesis layout

This thesis comprises six chapters and it is organized as follows; Chapter one is an introduction to the study. Chapter two describes the study area and data availability. Chapter three reports on an on a literature review about the subject matter. Chapter four describes the methodology applied in this research. In chapter five the results are shown and discussed. Chapter six finalizes the thesis by conclusion and recommendation

CHAPTER TWO: LITERATURE REVIEW

2.1 Introduction

Hydrologiska Byrans Vattenbalansavdelning (HBV) model is a semi-distributed conceptual model of catchment hydrology, which reenacts day-by-day flows utilizing daily temperature, precipitation, and estimated potential evaporation. The HBV model can be isolated into various vegetation and rise zones just as into various sub-basins and sub-catchments. The main two contrasts between HBV Light and different renditions are in the model initialization, which ought to be finished utilizing warming up period in HBV Light, and a directing parameter that can take every single real value rather than just whole number qualities (integers) Seibert et al., (2005). The HBV is a basic reasonable conception rainfall-runoff model, which is appropriate for various purposes, for example, simulating long streamflow records, streamflow gauging, and simulating the impact of environmental change as examined in detail section 4.3.2

2.2 Rainfall-Runoff modeling using HBV-light

The HBV model was developed at the Swedish Meteorological and Hydrological Institute to predict and simulate rainfall-runoff behavior by Forsman et al., (1973). Since that time, it became a standard tool for rainfall-runoff simulations in the Nordic countries and during the years the model faced a lot of modifications and the scope of application has also increased progressively. The HBV model can be named as a semi-conceptual theoretical rainfall-runoff model and depends on a sound physical premise as stated by Gardelin et al., (1997). As its developers state, the model is meant to be understandable for users and the number of free parameters should be kept to a minimum in order to prevent overparameterization.

Koutroulis, (2010) has conducted research on the application of the HBV hydrological model in a flash flood in Sola basin in Slovenia. This basin is a mountainous basin with a rising hill and steep slope. HBV Light model was calibrated and approved utilizing data from 01-January-2004 to 31-December-2007. The performance of the model was good and NSE ranging 0.82 to 0.96 for calibration and 0.47 to 0.90 for validation of all basins. Also, he checks for the coefficient of

determination R^2 and results were extending from 0.86 to 0.96 and 0.58 to 0.91 for adjustment and justification period individually.

Seibert, (2005) has performed the prediction on the uncertainty of conceptual rainfall-runoff models for identification model parameters and structure using the HBV model. With the help of the HBV model tool in Monte Carlo runs, a variety of parameter was allowed to vary while setting the range of a parameter (minimum and maximum). NSE of more than 0.85 was obtained at different parameter settings and after calibration NSE was varying from 0.825 to 0.876 at different parameter set which has indicated good performance of the model.

Anon, (2009) has modeled the river discharge for large drainage using the HBV model from lumped to a distributed approach. His focus was to check the model performance of the large basin for correlation between lumped and distributed model, and the model performed well in all cases. The basin was approximately 80657 km^2 covering the whole part of German. The model execution amid adjustment and approval was good for all case but with slightly better results in a distributed model where the performance criteria evaluated by the use of the coefficient of determination R^2. The performance R^2 for the lumped model were ranging from 0.65 to 0.79 for the period from 1985 to 1988 and 0.75 for whole period while R^2 for the distributed model were ranging from 0.77 to 0.88 for the period from 1985 to 1988 and 0.86 for the whole period. The HBV model has proven to give the best results regardless of the large basin area (80657 km^2) and low requirement of data input.

Zelalem & Mengistu, (2016) built up a new model where the HBV soil moisture idea was modified by new soil moisture routine, which estimates saturated and unsaturated volumes of underground water and with just a single parameter to calibrate, incorporated into the new model. The number of parameters to be calibrated in the module concerning soil moisture and overflow elements is reduced from seven in the HBV model to one in the new model. Anon, (2009) utilized the HBV model (version HBV Light 2.0) to discover the impact of the anticipated changes in precipitation attributes due to environmental change on the hydrological routine of the river Meuse. The hydrological demonstrate constrained with three high-resolution (0.088º) regional climate scenarios, each dependent on one of the three diverse IPCC CO_2 emission scenario for the time of

2002-2040 and 2062-2100. Their outcomes showed an abatement in summer release, due to the diminishing in the snowpack, and expanded discharge in winter.

Anon, (2007) has utilized the HBV Light model for appraisal of climate change impact on waterway flooding of the near future in the Suir catchment in Ireland. In the calibration, the number of parameters was calibrated to attain the good performance of the model. Calibration was done for five years and the coefficient of determination R^2 obtained was 0.787, which indicate good performance of the model.

Marofi et al., (2018) has performed research on assessment of the climate change impact on the hydrology and hydropower potential of a semi-arid basin by employing the HBV model in Dez Dam basin, Iran. Model calibration and approval were done utilizing the observed time series of the period not less than 20 years. The period of 15 years was selected for calibration and 5 years for validation and the results were obtained as follows, for calibration period NSE for all sub-basins were ranging from 0.62 to 0.68 and coefficient of determination R^2 was ranging 0.62 to 0.70. In the validation part, the NSE was ranging from 0.43 to 70 and the coefficient of determination R^2 was ranging 0.60 to 0.79 which has indicated the acceptable performance of the model.

Anon et al., (2007) assessed the hydrological response to climate change on the Ourthe catchment using HBV model. The model was evaluated using observed daily data obtained from weather stations and gauging station, although data were spinning with a different period. The model has shown the best performance since the result obtained during calibration and validation was good. The calibration result was 0.84 for NSE and coefficient of determination 0.86 was obtained whereas for validation results were 0.89 and 0.90 for NSE and coefficient of determination R^2 respectively.

Beven et al., (2009) made the prediction on the number of discharge measurement needed on the ungauged catchment in order to improve the hydrological response of ungauged catchment using HBV model. Elevation catchment was select as a case study, all catchments were located in central Sweden north of Uppsala. The performance of the model was evaluated based on a different subset

and performance criteria. For most of the catchment during calibration the model efficiency (NSE) was tested for 10 years with a daily time step, the catchments performance from the model, NSE was 0.8 for the most catchment, 0.85 for three catchments, and 0.70 for rest two catchments.

Booij et al., (2004) surveyed the effect of climate change on waterway flooding with various spatial model resolution in the Meuse basin using HBV model. The catchment was modeled using different spatial model resolution (HBV-1, HBV-15, and HBV-118) to identify the effect of the resolution on model results. Parameter estimation was done for HBV-1 and HBV-15 using previous studies as the startup and then after sensitive analysis were checked using Monte Carlo runs. Regionalization of the parameter for HBV-15 and HBV-118 were estimated using multiple sensitive analysis and Monte Carlo analysis. The model performance during calibration and validation was evaluated based on the coefficient of determination R^2 and difference in discharge (RVE) between observed and simulated. At the time of calibration, R^2 was 0.85, 0.87, and 0.88 for HBV-1, HBV-15, and HBV-118 respectively and RVE were 0 for HBV-1, +4 for HBV-15 and +1 for HBV-118. The model showed the best performance during validation with R^2 of 0.91, 0.92, and 0.93 for HBV-1, HBV-15, and HBV-118 respectively and RVE were +1, +4, and +2 for HBV-1, HBV-15, and HBV-118 respectively. The model has shown the best result at all resolution but it has revealed that performance increase as the resolution increases. (HBV-1(150 km), HBV-15 (40km), and HBV-118 (13km)

Leibundgut et al., (2009) has predicted uncertainty of conceptual rainfall-runoff model by use of the HBV model that can be caused by a problem in identifying model parameters and structure in Brugga basin, Germany. Their main focuses were to analyze parameters which affect many models during simulation in order to determine their uncertainty according to basin or catchment characteristics varying from one to more parameter set at a time. Monte Carlo procedures were used to investigate the uncertainty of parameters. The parameter shown good performance during Monte Carlo runs with the model efficiency of more than 0.85 for all 400,000 runs. Due to the application of different variant during investigating uncertainty of parameters of the model, it is revealed that the more linearity on each response function box of the HBV model attains good results. Also in addition to that, the more model is distributed to improve the results and more precise prediction.

Lyon et al., (2017) utilized global precipitation dataset in the limited regions for comparison using different global data set and a different method of bias correction at Kilombero Valley in Mpanga catchment. HBV model was used to run different data set from the global dataset and thereafter data were corrected using a different method of bias correction and rerun again to identify its effects with respect to produced results. The diverse worldwide dataset has indicated distinctive outcome, and these results have improved when distinctive methods of bias correction applied. Distinctive methods of bias correction applied were Quantile Mapping (QM), which utilizes daily resolution GPD product only, Daily Percentages (DP) which utilizes monthly resolution GPD product only, and a Model-Based (ModB) predisposition amendment utilizing HBV model, which utilizes for both daily and monthly resolution GPD product. The model outcomes were genuinely great before predisposition amendment and were quite improved after bias correction. Prior to predisposition adjustment, the model productivity NSE were extending from 0.38 to 0.63 while after bias correction was running from 0.57 to 0.68. Concerning predisposition bias correction methods, Model-Based (ModB) bias correction gives a good outcome contrasted with rest techniques applied.

Jones, (2017) surveyed the vulnerability of climate change impacts on Southern Alps stream utilizing the HBV model and TopNet to explore the job of the hydrological model and its multifaceted nature. Amid utilization of both all model, he finds that TopNet is increasingly complex in model structure and interphase contrasted with HBV model. Despite the fact that TopNet is progressively convoluted however, the outcomes as far as the model proficiency was appeared to be the same, where NSE for HBV model was 0.72, while for TopNet was 0.71. Despite the fact that the HBV show looks easy to utilize and require little data input, delivers the best outcomes contrasted and another model as above HBV results are marginally higher than the TopNet model.

Bronstert et al., (1999) modeled the river discharge for large drainage using the HBV model from lumped to a distributed approach. His focus was to check model performance for the large basin and compare with lumped and distributed one, but the model performed well in all cases. The basin was approximately 80657 km^2 covering the whole part of German. The model performance during

calibration and validation stage was good for all case but with slightly better results in a distributed model where the performance criteria evaluated by the use of the coefficient of determination R^2. The performance R^2 for the lumped model were ranging from 0.65 to 0.79 for the period from 1985 to 1988 and 0.75 for whole period while R^2 for the distributed model were ranging from 0.77 to 0.88 for the period from 1985 to 1988 and 0.86 for the whole period. The HBV model has proven to give the best results regardless of the large basin area (80657 km^2) and low requirement of data input.

Merz, (2010) has performed the application of HBV model to the Tamor Basin in Nepal to predict runoff at the outlet of the basin. Calibration and validation of the model were done utilizing the data recorded at Mulghat with a spinning period of 01-01-1987 to 31-12-1996. The performance criteria selected during calibration were Nash Sutcliffe Efficiency NSE, and coefficient of determination R^2 whose values were 0.693, 0.689, and 0.649 for GAP optimization, focus on low flow and focus on high flow respectively and 0.692, 0.680, and 0.622 as NSE values for GAP optimization, focus on low flow and focus on high flow respectively. The model has shown good performance for all case above as was applied for discharge estimation at Tamor basin. With regard to the mode application, the HBV model becomes the best tool for discharge estimation for large and small catchments due to its high applicability, low input data requirement and easily understandable.

Johansson, (2009) has made a review on the improvement of the HBV model for rainfall-runoff at river Rhine. The model performed well in all cases but less when incorporated with FEW systems. The longer period of calibration and short time of warming up the model for simulation purpose has managed to predict properly the runoff. The performance criteria for the model were R^2 and R^2 log, which looked similar during evaluation in all basins. The R^2 for the model in all six basins were ranging from 0.88 to 0.92 and R^2_{log} were ranging from 0.78 to 0.90 with a marginal difference. The overall result was good as the R^2 and R^2_{log} for all basins were more than 0.80 after recalibration, which reveals that the model has managed properly, predicted the runoff at the outflow with the high performance of more than 80%.

2.3 Climate change impact on hydrology

Sarukkalige et al., (2017) utilized the conceptual rainfall-runoff model to survey the effect of climate change on hydrological behavior of catchment. He used HBV light model as the tool of simulating and predicting the response of Richmond catchment for the near future (2016-2043), middle future (2044-2071) and far future (2072-2099). Future atmosphere data was extracted from the Global Climate Model (GCM) of the Coupled Model Intercomparison Project Phase 3 (CMIP3) with three local atmosphere scenario, A2, A1B, and B1. The general outcome for all GCM demonstrated that they would be marginally expanded in precipitation amid the near future and diminishing amid the mid future. Additionally, he found that they will be a critical difference in the catchment as most extreme and least streamflow are expected to diminish later on in all scenarios

.

Roy et al, (2003) evaluated the impact of climate change on streamflow in the Mississippi river basin using Regional climate model (RCM) incorporated with the hydrologic model, the Soil and Water Assessment Tool (SWAT). With the utilization of observed streamflow data available, the SWAT model was adjusted and approved. The RCM and SWAT performed well on a yearly basis for streamflow estimation. In view of future forecast, the model demonstrated that the precipitation will increment by 21% while streamflow increments by 51%. More parameter was assessed and the model has appeared 43% expansion in groundwater recharge coming about water yield increment by 50% while 18% expansion in snowfall.

Rozeana et al., (2015) conducted a research on changes in river flow due to climate change impact on Brunei River, He uses WEAP model combined with GIS with different four scenarios based on land use change, the growth of industry and climate change based on prolonged wet climate categorization. His main focus was to assess vulnerability to flooding due to increased wet season in the catchment. The previous study analysis for data collected for more than 45 years has shown that there is an increase of average rainfall at a rate of 1.33% per year, a number of wet days 0.16 days/year and temperature 0.0375^{o}C per year. Also, he has narrated that over 105 landslides and 115 cases of flooding events were reported in 2014 alone. The catchment has shown to be more vulnerable to flooding under an extended wet period resulting in the creation of a detention pond

near the river. This presumed that after few next years to come river flow be significantly altered and the whole drainage could be almost inundated by water, which can result in the wetland.

Kebede, (2017) investigated the effect of climate change on the water assets in the Megech River Catchment, Ethiopia. He utilizes HBV light model to simulate and forecast the stream flows with a combination of the large scale regional climate model (REMO) and its yield was downscaled statistically to metrological factors at daily resolution utilizing SDSM model. However, the execution of the HBV model was great amid adjustment and approval were NSE of 0.91 and 0.86 were obtained individually. On his discoveries found that the mean most extreme temperature with expanding pattern going from +0.1˚C to +0.51˚C and +0.12˚C to +0.57 for scenario A1B and B1 individually of the period 2015 to 2050. Meanwhile, the mean minimum temperature demonstrated a diminishing pattern going from −0.11˚C to −0.61˚C and −0.12˚C to −0.60˚C for scenario A1B and B1 individually for the future time horizon from 2015-2050. Amid his examination, there is no reasonable pattern of precipitation since rising and falling pattern was noted over the whole catchment. The mean monthly precipitation indicated both expanding and diminishing pattern with a range of +6.7% to +34.5% and +11.0% to +38.89% and −1.14% to −31.88% and −1.6% to −36.42% for A1B and B1 scenario respectively of things to come period from 2015-2050. For the hydrological response of the catchment, they will be the decline in peak streamflow of about (−17.47% to −30.58%) for August and September, which could prompt a reduction of discharge.

2.4 Research gap in the study area

The number of studies has been carried out in Tanzania particularly in water resources; hydrological modeling and simulation are inconclusive. They highlighted the increase in water demand due to population growth, change of land use land cover and urbanization in coming years while not providing the linkage of change of climatic variables such as temperature and rainfall with discharge variability. Change of climate conditions has a great impact on water assets and the ecosystem.

Xu, (2005) has shown that the availability of water resources is greatly affected by climatic conditions that may vary with decadal, seasonal and inter-annual times series. However, modeling

and simulation of the watershed with a climatic variable as inputs play an important role in understanding climate change through the linkage of change of climatic conditions and water resources availability. Therefore, hydrological modeling and simulation at Malagarasi catchment using climatic variables at different climatic scenarios for prediction of river (stream) flow at the outflow will provide linkage between the change of climatic variables in estimation available water in the catchment. Furthermore, a detailed analysis of the change of climate variables linkage with river (stream) flow must be addressed in water resources management plans for the future adaptive measure.

CHAPTER THREE: STUDY AREA

3.1 Location

Malagarasi catchment is among the catchments those drain into Lake Tanganyika basin and is located in the western part of Tanzania between latitudes 2^0 45″ and 5^0 42′ and longitudes 29^0 35′and, 33^0 40′. The total catchment area of the basin is 67112.5km^2. The catchment comprises around 33% of the catchment area of Lake Tanganyika basin and contains biological communities of both national and global significance (for example Muyovozi Wetland Ramsar Site) as can be seen underneath figure 3.1.

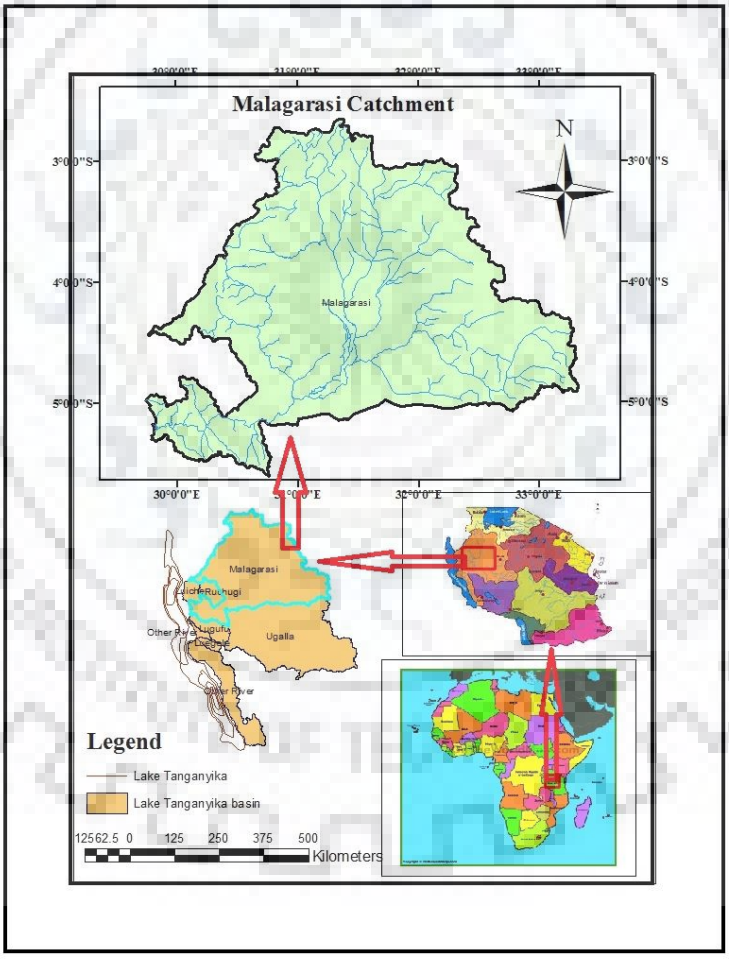

Figure 3.1: Location of Malagarasi catchment

3.2 Climate

The climate of the catchment is semi-humid tropical climate with two fundamental seasons that is the dry season from June to October and the wet season from November to May. Air mass movement along the precarious incline or bluff produces frequent intense rainfall in highly localized heavy rainstorms especially in areas of north Kigoma (LTBWB, 2011)

3.3 Temperature

The temperature in the basin range from 19 ^{O}C to 30 ^{O}C, the average temperature around Malagarasi catchment is 23 ^{O}C. The variation in mean monthly temperature is small, while the spatial variation is much larger and is related to altitudinal differences (LTBWB, 2015a).

3.4 Topography

The catchment is a tenderly slanted level with steep slopes rising very sharply from 773 m at the level of Lake Tanganyika to heights of 1, 800 m toward the East slipping from the North and East into delicately moving slopes with major perennial rivers of Malagarasi. This river comprises the major drainage area.

3.5 Drainage Pattern

The Malagarasi catchment is the largest catchment in the basin, covering nearly 67113 km^2 and drains approximately 30,000 km^2 of the Kigoma region. Additionally, the river drains 93,300 km^2 of Burundi and Shinyanga, Tabora, and Rukwa Regions in Tanzania. The river begins in the mountainous landscape area near the border of Tanzania and Burundi at an altitude of 1750 m.a.s.l from where it runs northeasterly through the hilly and mountainous landscape and then Southwards into flatter area east of the Kasulu – Kibondo Road. Due to the low gradient in this reach, the river flows in large meanders before entering the Malagarasi swamps in the southeast.

3.6 Land Use/Cover

The vegetation in the zone comprises of upland vegetation, which incorporates shut and open forest, bramble land brush, ragged meadow, marsh or wetland vegetation comprising of lush field and bogs. Forest is the normal vegetation over the vast majority of the basin and can be isolated

into two groups: Miombo forest and Acacia, Combretum and Albizia species. Bushland bushed field and uncovered land considered being a debased type of various diverse vegetation types which have been cleared, consumed, perused and specifically nibbled for a long time are the most boundless sorts in the basin with the extreme condition in the Eastern part of the Basin where tobacco cultivating has been drilled over years. Subsistence cultivating of sustenance crops for example banana, maize, cassava, beans, and season paddy rule the region, in marshes along with the Lake Tanganyika shore palm oil rule the territory.

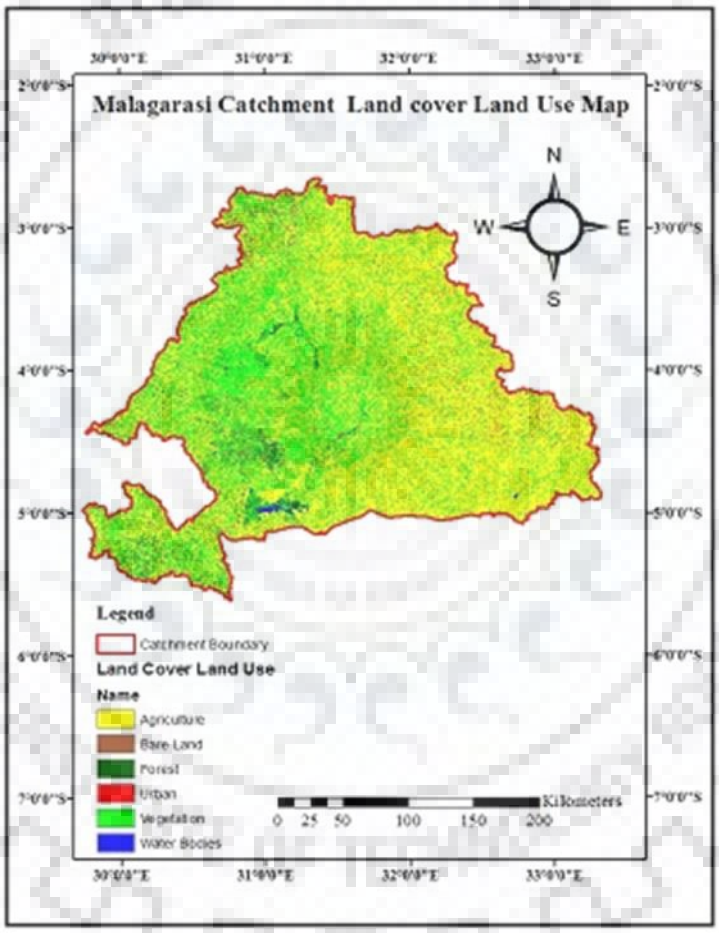

Figure 3.2: Map of land use the land cover distribution in the catchment.

3.7 Soils

The soils of the basin can generally be categorized as follows: Along the lakeshore, the soils are profound and very much depleted containing the dull ruddy darker fine sandy soils, sandy topsoils,

and most seriously eroded areas, indicating stony outcrops. The overwhelming dark soils are found in perpetual waterlogged regions with dark clayey soils, which have a high extent of sand in marsh borders subject to occasional waterlogging. These are an exceedingly fertile zone in view of the high extent of sand and residue. Nevertheless, these soils are not exposed to occasional wetting and drying like the cotton soils in light of the fact that the water table is high. In the low relief areas, the soils are dark reddish clay loams with great inner seepage while the dark and darker alluvial soils are generally found in zones of high relief. On the west of the basin, soil varies widely, ranging from sandy loam to heavy (black/dark brown) soils in poorly drained areas especially in the Northern part of Tabora region.

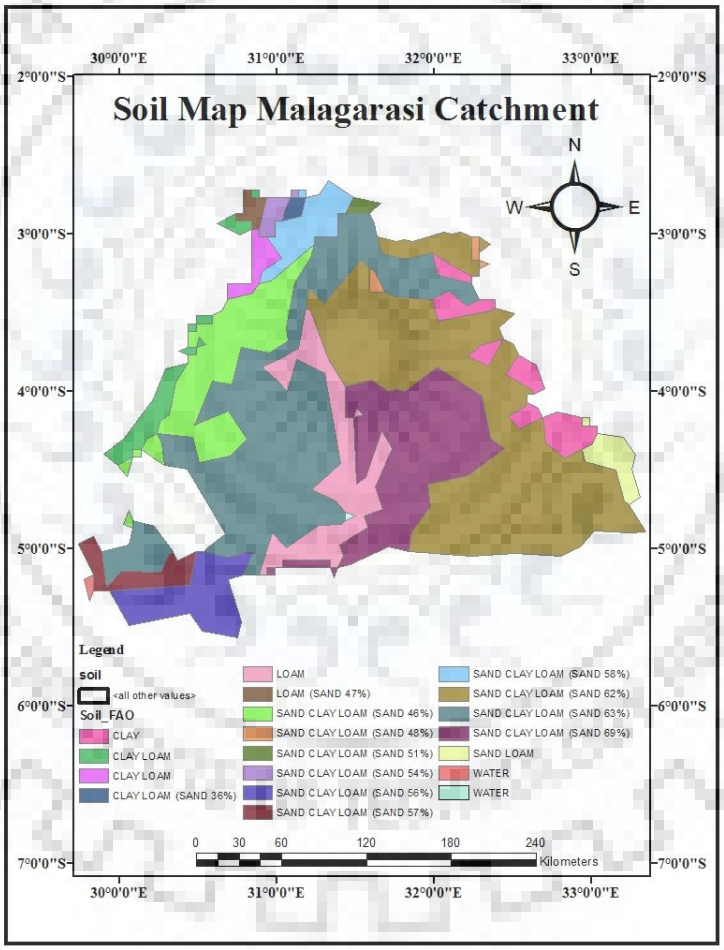

Figure 3.3: Soil Map of Malagarasi Catchment

3.8 Geology

The geology of Malagarasi catchment comprises of oldest rocks of the area are gneisses and schists, which occur in the northwest and irregularly along the shores of the Lake Tanganyika toward the south (SMEC, 2014). The rocks are exactly similar in type to rocks of the Ubendian system. They represent an ancient series of sediments, probably shale, sandstones, and greywackes, which have altered by regional metamorphism and migmatization to their present high grade. Overlying these rocks with unconformity is the Kigoma quartzite. This thick formation consists almost entirely of coarse-to-medium grained, white, occasionally, cream, pure quartzites, and sandstones, with occasional bands of quartz pebbles. There are few horizons of shaly beds, which often show signs of shearing, and thin basal conglomerates are sometimes developed as can be seen in figure 3.4 below.

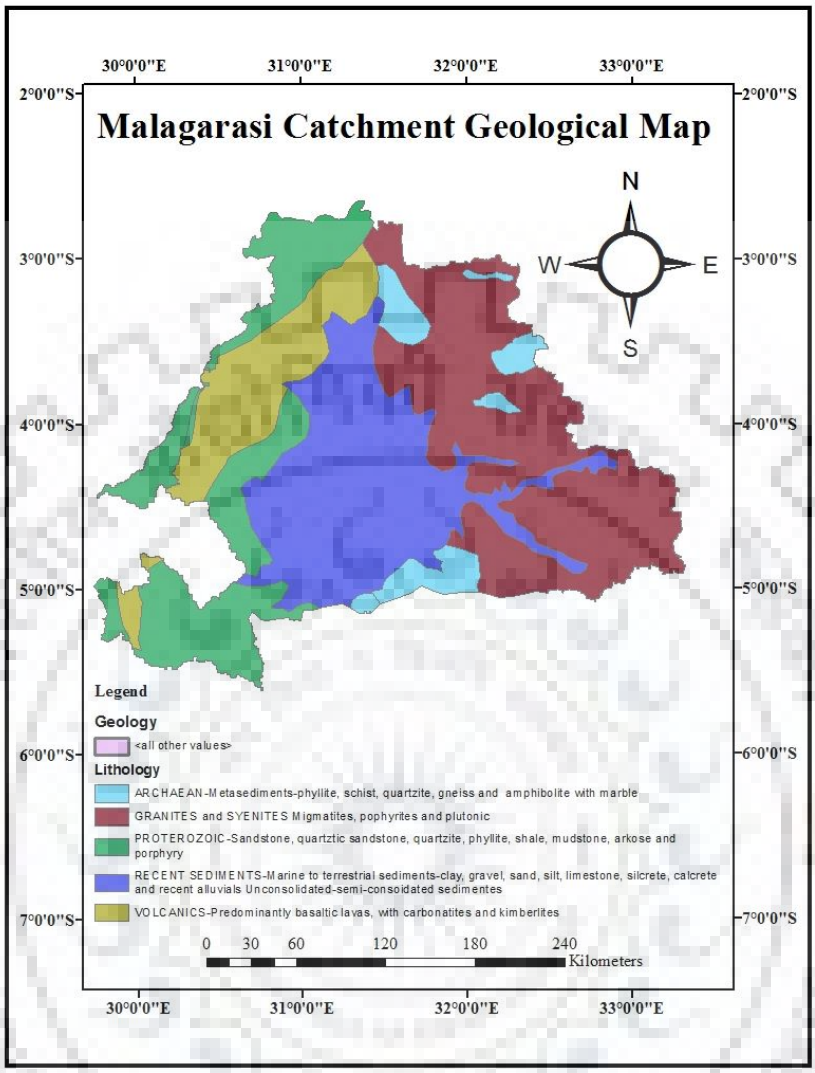

Figure 3.4: Geological Map of Malagarasi Catchment

3.9 Reservoirs/Lakes Information

3.9.1 Lakes Information

Existing Lakes include the famous Lake Tanganyika and the satellite lakes of Nyamagoma and Sagara which are located within the Malagarasi Moyowosi Wetland. The two satellite lakes function is mainly to serve as detention buffer feeding Malagarasi River. According to SMEC (2013), the Satellite Lake levels rise by 1 to 1.5m during the wet season as compared to the dry season, however progressively the Lake sizes have been shrinking from one year to another.

3.9.2 Artificial Reservoirs Information

The Basin has 35 man-made reservoirs which have a capacity of storing about 50,313,400 m^3**.** Among the artificial storages include Kazima, Igombe and Shunu dams. Kazima and Igombe dams shown in figure 3.5 below occupy 45,122,000 m^3 which are 90% of the whole man-made storages in the Basin, the two reservoirs were purposely constructed to save for domestic water use for Tabora Municipality and its suburbs.

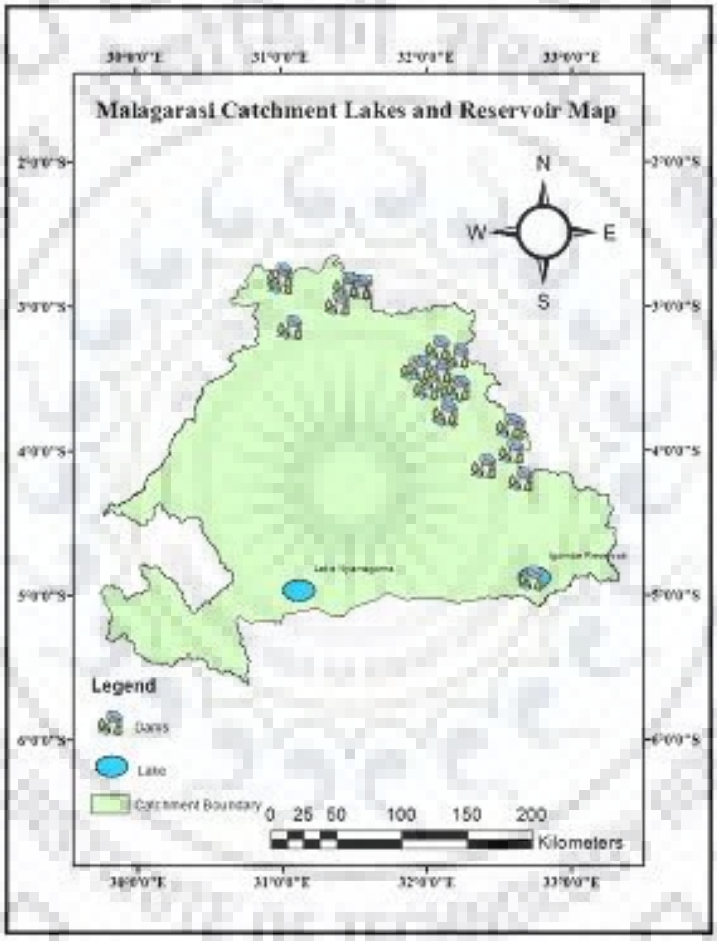

Figure 3.5: Lakes and reservoir

3.10 Data used.

3.10.1 Digital Elevation Model

Digital Elevational Model was extracted from NASA which accommodates DEMs for the whole globe. DEMs with a spatial resolution of 30m by 30m was acquired from the site (https://earthexproler.usgs.gov) in GeoTIFF format. DEM of Malagarasi catchment is shown in figure 3.6 below.

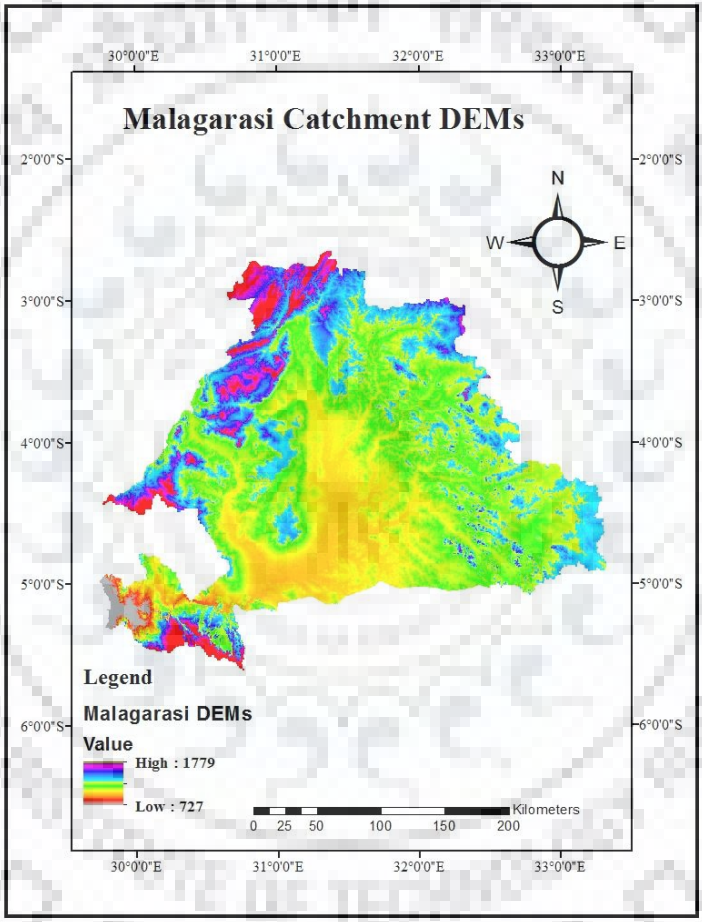

Figure 3.6: DEM of Malagarasi Catchment

3.10.2 Hydrometeorological data

Most of the hydrometeorological stations in Lake Tanganyika basin were established in the early 1960s and the records are available. In the last 20 years, there were about 17 hydrometric stations, 18 rainfall stations and 85 weather stations of which 27 fall under Malagarasi catchment. There is

a lack of useful hydrometric data for a period of 1998 to 2009 in most of the stations, as most of the stations were inoperative during this period. From 2009 onward many of the stations were rehabilitated and improved. Others were realized during the study of IWRMD under international consultancy agency, Single Module Engine Controller (SMEC) study team in collaboration with lake Tanganyika water basin staffs. The list of stations shown in Table 3.1 below with respects to location

Table 3-1: Rainfall and Temperature gauge network.

Station Name	Station ID	Elevation (a.m.s.l.)	Latitude	Longitude	Missing Data (%)
Runazi **	9231005	1402	-2.78	31.48	15.1
Nyakahura *	9231006	1432	-2.8	31.07	18.7
Runazi Primary School **	9231016	999	-2.78	31.47	12.7
Kibondo Mission **	9330000	1518	-3.58	30.7	8.1
Kakonko Primary School *	9330002	1219	-3.28	30.95	7.9
Kibondo District Office **	9330005	1515	-3.57	30.67	9.7
Kakonko **	9330006	1463	-3.3	30.93	12.9
Kibondo Maji Depot **	9330007	999	-3.6	30.72	13.5
Ushirombo Mission **	9331001	1188	-3.47	31.88	18.2
Buseresere *	9331004	1219	-3.07	31.88	17.6
Mawe Meru Mine **	9332001	999	-3.22	31.65	15.5
Mulera Primary School *	9429000	1417	-4.43	29.95	15.1
Makere Primary School **	9430002	999	-4.28	30.42	9.2
Kagera Mission **	9430005	1097	-4.67	30.67	14.1
Kabanga **	9431000	1036	-4.92	31.45	13.9
Uyowa **	9431001	999	-4.5	31.75	8.7
Bulombora Nat.Service **	9529002	999	-5.03	29.78	11.4
Uvinza **	9530000	990	-5.13	30.38	10.2
Malagarasi Railway Stn *	9530002	1060	-5.12	30.85	9.2
Uvinza Salt Mine **	9530006	991	-5.12	30.37	25.2
Kazima Dam **	9532014	998	-5.02	32.08	18.9
Tabora Maji (W.D.& I.D. **	9532024	1021	-5	32.07	15.7

*Double stars ** indicate rainfall and temperature and single star *, indicate rainfall gauge station only.*

Daily rainfall and flows data acquired from the Ministry of Water and Irrigation, Lake Tanganyika Basin Water Board and some daily rainfall data were acquired from the national meteorological office of Tanzania. The estimated monthly mean climate potential evapotranspiration values estimated by Hargreaves and Samani (HS) formula employing maximum and minimum air

temperature. Thiessen polygon was used to apportion weights to rain and temperature stations for input in the HBV model and its outputs were shown below in figure 3.7 and table 3.2

Table 3-2: Thiessen Polygon areal distribution

Station ID	Latitude	Longitude	Shape Area	Thiessen Polygon ratio
9231005	-4.28	30.42	6579.50	0.0980
9231006	-4.5	31.75	7415.82	0.1105
9231016	-3.22	31.65	6308.57	0.0940
9330000	-3.6	30.72	8885.61	0.1324
9330002	-5.12	30.85	5416.91	0.0807
9330005	-5.13	30.38	3413.20	0.0509
9330006	-5.03	29.78	1319.05	0.0197
9330007	-4.45	29.93	700.72	0.0104
9331001	-4.58	32.08	4437.09	0.0661
9331004	-4.05	32.02	3899.28	0.0581
9332001	-5	32.07	3971.91	0.0592
9429000	-4.16	32.24	8013.83	0.1194
9430002	-3.07	31.88	630.31	0.0094
9430005	-3.47	31.88	4857.66	0.0724
9431000	-3.05	32.05	1263.02	0.0188
Sum	**NA**	**NA**	**67112.48**	**1.0000**

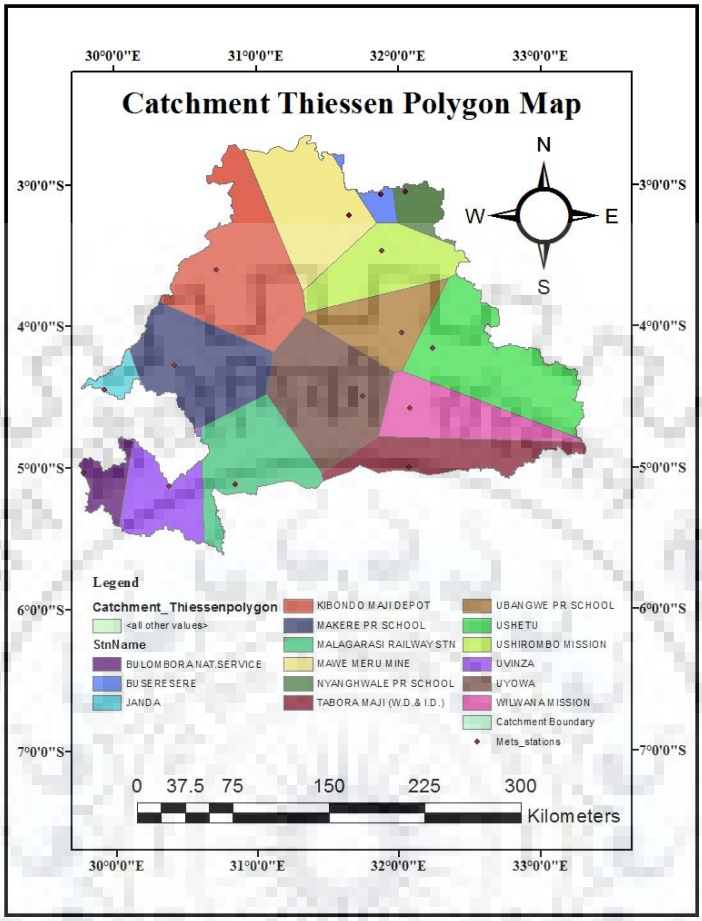

Figure 3.7: Thiessen polygon areal distribution

3.10.2.1 Rainfall

Daily rainfall data have been obtained from meteorological stations inside or in the region of the river basin figure 3.7 above for the time of 1960's till date with some gaps in most of the months. In this investigation rainfall data utilized was from 2000 to 2015. The obtained data was then inter- and extrapolated on a spatial raster over the entire basin to generate areal mean values. Given the accessible information, Thiessen polygon is utilized to acquire the areal mean estimation of rainfall. Table 3.2 demonstrates that the meteorological stations unevenly appropriated over the catchment and section 3.2, 3.3, and 3.4 demonstrates that the Malagarasi catchment is a genuinely comparative territory concerning yearly mean rainfall, rise, and climate. In this manner, an investigation was performed to locate a fitting way to deal with ascertain the areal mean precipitation as have found in figure 3.7 using Thiessen polygon.

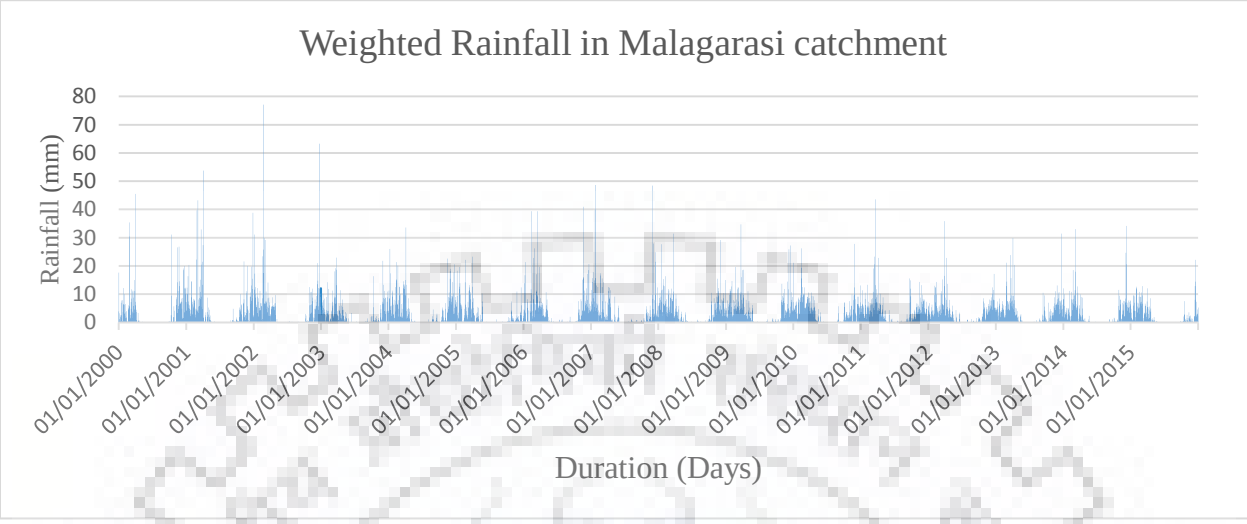

Figure 3.8: Observed Rainfall (2000-2015)

3.10.2.2 Discharge station

The Malagarasi River catchment is a smaller in the area of about 67112.48 km^2 compared with Mamoré River with a basin area of (240000km^2), where it was desirable to divide the basin into several sub-basins. The Mamoré River basin was partitioned into three sub-basin: Ichilo sub-basin (7900 km^2), Grande sub-basin (53300 km^2), and Rio Mamoré sub-basin 61400 km^2 (W.H. Maat, 2015). Therefore, for Malagarasi catchment was treated as a single catchment.

Discharge measurement at the outflow of Malagarasi catchment at Malagarasi Mberagule station 4A9 was started early 1970's. Most discharge measured were made seasonally during low flow, medium flow, and high flows. Due to this, there were no daily discharges but seasonal discharge. Only water levels at Mberagule station were recorded daily in the morning at 9:00 am, and evening time at 5:30 pm till date. Few seasonal discharge data set available were used to develop a rating curve for the generation of daily discharges. In this study, data was used from 2000 to 2015. Long-term observed discharge data at Mberagule station were missing. The hydrograph is shown in figure 3.9.

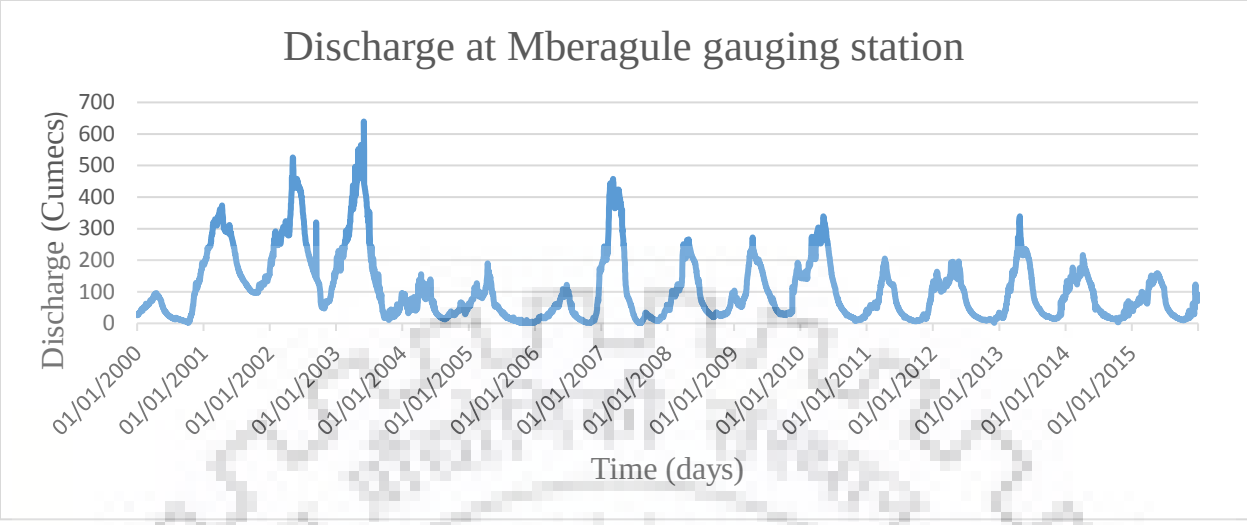

Figure 3.9: Observed Discharge (2000-2015)

3.10.2.3 Temperature

Daily maximum and minimum temperature data collected from all weather stations over the entire catchment. Daily averages of maximum and minimum temperatures were computed, and using Thiessen polygon in figure 3.10 temperature data from all stations were weighted to get a representative for the catchment.

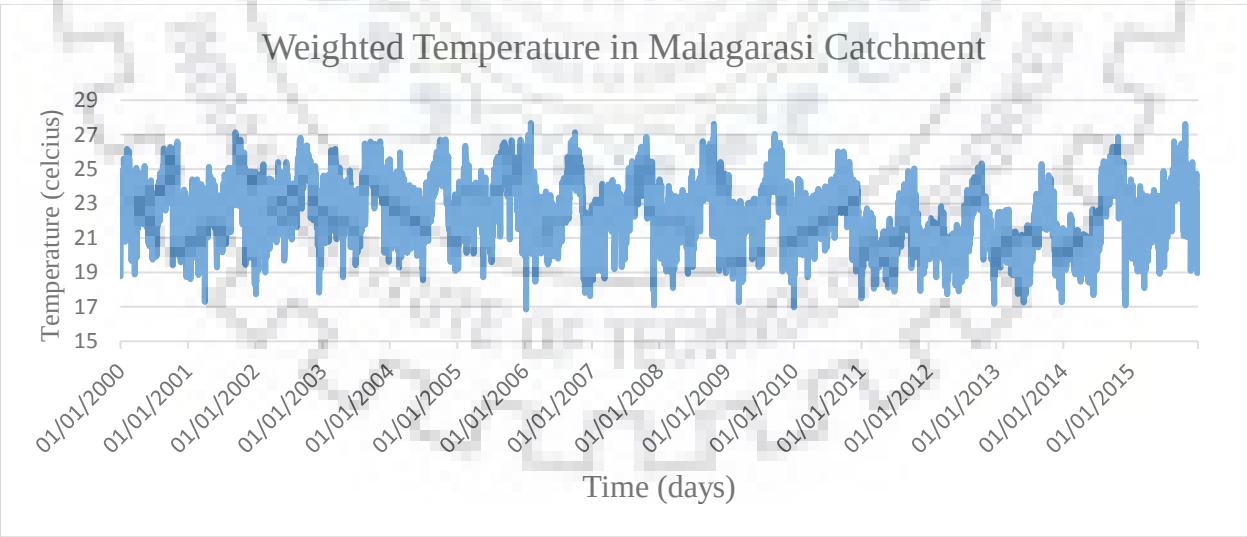

Figure 3.10: Observed Temperature (2000-2015)

3.10.2.4 Potential evapotranspiration

The estimated monthly mean climate potential evapotranspiration values used to drive the HBV model were estimated by Hargreaves and Samani (HS) formula. Although the recommended formula for potential evaporation estimation is Penman-Monteith, due to its relatively high demand of parameters such as wind speed, humidity, solar radiation incorporated with aerodynamic aspect and thermodynamic which are observed at relative few in Africa weather stations, this method was not used. The most available parameters in developing Africa countries are maximum and minimum temperatures and rainfall. The use of Hargreaves and Samani (HS) formula require only mean maximum, minimum air temperature and extraterrestrial radiation for estimation of potential evapotranspiration. The formula has ranked the best among methods, which require air temperature data only. The Hargreaves-Samani (HS) formula can be defined as

$$ET_O = 0.0023 * 0.408 * Ra\,(T_{mean} + 17.8)\sqrt{T_{max} - T_{min}} \qquad (3\text{-}1)$$

where ET_o is the monthly averaged reference evapotranspiration (mm day^{-1}), R_a is the extraterrestrial radiation (MJm^{-2} day^{-1}), T_{mean} is averaged monthly temperature (^oC), and T_{max} and T_{min} are maximum and minimum monthly temperature (^oC). The monthly evapotranspiration (ET_o) is obtained by multiplying with the number of days in the month. The potential evapotranspiration is calculated by multiplying ETo with the crop factor, K_c

$$ET_P = K_c \text{ x } ET_o \qquad (3\text{-}2)$$

The yield factor depended on vegetation cover of the Malagarasi catchment, which was given by ESA Climate Change Initiative (CCI) land cover database updated lastly on 2017. The Malagarasi catchment is partitioned into five land cover types, each with the explicit crop factor, agricultural land (1.03), bushes (1.16), urban zone (1.0), forest (1.19), uncovered land (1.05), and grassland (1.02). Multiplying each of surface area fraction with the corresponding crop factor, the resultant average crop factor obtained was (1.07). With this overall improvement, reasonable potential evapotranspiration values are estimated using incoming extraterrestrial radiation and air temperatures. The estimated potential evapotranspiration is shown in figure 3.11 below

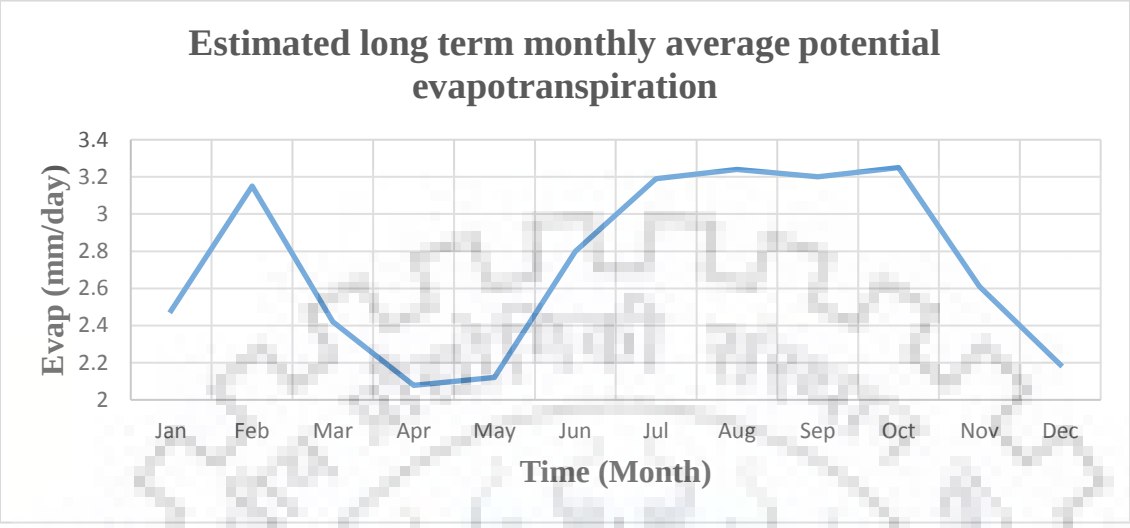

Figure 3.11: Estimated monthly mean potential evapotranspiration

CHAPTER FOUR: MATERIAL AND METHOD

4.1 Material

4.1.1 Digital Elevation Model

Digital Elevation Model was downloaded from NASA website. DEMs with a spatial resolution of 30m by 30m was downloaded from the site (https://earthexproler.usgs.gov) Aster Global DEMs in GeoTIFF format.

4.1.2 Landsat Image

Different Landsat Images were extracted from NASA website. The land sat image extracted from NASA were of different periods, three consecutive years of 2015, 2016, and 2017 were extracted for assessing land use a land cover over the catchment.

4.1.3 Geological and soil maps

Geological and soil maps were obtained from the Ministry of Energy and Minerals of Tanzania. This helps to understand catchment soil and geology distribution over the catchment as underlying rock and soil in the catchment play an important role in groundwater estimation.

4.1.4 Software and program used

i. Geographic information system (GIS)
ii. Erdas Imagine
iii. HBV Light Model
iv. R Studio
v. Statistical Down-Scaling Model (SDSM)

4.2 Data analysis

4.2.1 Statistical evaluation and model performance

A different number of the statistical parameter have been accepted for model performance in hydrological modeling, but few of them have been accepted worldwide to be used for model

acceptance. These include Nash-Sutcliffe efficient (NSE), the coefficient of determination (R^2) and percent of bias (PBIAS). Ritter, (2013) stated that the use of a computer model for simulating environmental variables requires model calibration and validation procedures. Using NSE for evaluating the goodness of fit for the model may be subjective. It is important to consider more than one statistical parameters in model performance in order to avoid biases. In further extent employing visual inspection before statistical parameter acceptance is better since all statistical parameter may fail to represent the extreme events and outliers. NSE measure the goodness of fit between observed and simulated values. NSE value may range from ∞ to 1, with 1 being a perfect fit while 0 indicating a poor match between modeled and observed. Negatives values indicating model prediction is worse and in hydrological modeling, NSE of at least 0.7 is considered good. The NSE equation is given by

$$NSE = 1-\left[\frac{\sum_{i=1}^{n}(Y_{obs}-Y_{sim})^2}{\sum_{i=1}^{n}(Y_{obs}-Y_{mean})^2}\right] \quad (4\text{-}1)$$

Where

Y_{obs} = the observed values

Y_{sim} = the simulated values

Y_{mean} = the mean of the observed values

The NSE can be chosen, as the best indicator of the model evaluation even though needs another supportive statistical parameter to conclude conclusively. It has stated that drawback of NSE is more difficult to achieve high values making less attractive for the first views (Krause, 2005).

The percent of bias (PBIAS) measures the tendency of being over or underestimate of simulated values with the observed values. The optimal values of PBIAS are 0 while negative values indicating overestimation and positive values indicating under-estimation bias. The equation is given by

$$PBIAS = \left[\frac{\sum_{i=1}^{n}(Y_{obs}-Y_{sim})*100}{\sum_{i=1}^{n}Y_{obs}}\right] \quad (4\text{-}2)$$

Where these variables are similar to those of NSE

The coefficient of determination (R^2) values describes the degree of fit of modeled and observed data. The R^2 assess how well a model explains and predict future outcomes based on modeled and simulated data. It is stated that one way of interpreting R^2 is to say that the variables included in a given model explain approximately a certain percent of the observed variation, which can be used to measure the model accuracy. In some literature $R^2 \geq 0.5$ can be satisfactory to accept the model (Kenton, 2019).

The equation of R^2 is given as

$$R^2=\left(\frac{(n\sum_{i=1}^{n}\mathrm{Y_{obs}}-\mathrm{Y_{sim}})-(\sum_{i=1}^{n}\mathrm{Y_{obs}}*\sum_{i=1}^{n}\mathrm{Y_{sim}})}{\left(\sqrt{((n\sum_{i=1}^{n}{Y_{obs}}^2)-(\overline{Y_{obs}})^2)}\right)*\left(\sqrt{((n\sum_{i=1}^{n}{\mathrm{Y_{sim}}}^2)-(\overline{Y_{sim}})^2)}\right)}\right) \quad (4\text{-}3)$$

Where

$\overline{Y_{obs}}$= the mean of observed values

$\overline{Y_{sim}}$ = the mean of simulated values

4.2.2 Sensitivity analysis

In HBV Light model, there are 15 parameters that need to adjust in order to achieve an acceptable range of model performance. These parameters are grouped into five categories, which includes snow routine, soil moisture routine, response routine, routing routine, and others. Using GAP optimization, a number of parameters were set in an acceptable range varying at each run. More than 100,000 runs were chosen to study sensitivity analysis of all parameters. Some of the parameters were not sensitive at all especially from snow routine since in the area of study there is no snow and some are less sensitive and others were most sensitive especially found in response and soil moisture routine. These most sensitive parameters include FC, BETA, LP, PERC, K1, and K2. The variation was 40% higher or lower of the calibrated parameters.

4.2.3 Climate change impact assessment

Global weather climate variables used as predictors were obtained from the site (http://www.ipcc-data.org/sim/gcm_monthly/AR5/Reference-Archive.html) with different resolutions. Four GCM

were selected with a daily time step, which includes CSM1.1, BNU, CanESM2, and MIROC. In each GCM, RCP 4.5 and RCP 8.5 scenarios were selected at daily time steps in which four predictors were extracted for prediction of rainfall, maximum and minimum temperatures, which includes air temperature (tas), convective precipitation flux (prc), relative humidity (rhs) and specific humidity (huss). All predictors were from 2006 to 2099 or 2100 depending on GCM calendar settings. Data Distribution Centre (DDC) under the Intergovernmental Panel on Climate Change (IPCC) provides data and reports regarding present and future climate. Only four GCMs were selected from IPCC-DDC, although more GCMs are recommended, due to the time step of the data required by HBV model (daily data), having common climate change scenarios of RCPs 4.5 and 8.5, and spinning with the same past to future predictor variables.

Table 4-1: Four Models selected from CMIP5 experiment

Centre(s)	**Centre Acronym(s)**	**Model**	**Scenario (Rcp)**
Beijing Climate Center, **China**	BCC	BCC-CSM1.1	rcp4.5 & rcp8.5
Beijing Normal University, **China**	BNU	BNU-ESM	rcp4.5 & rcp8.5
Canadian Centre for Climate Modelling and Analysis, **Canada**	CCCma	CanESM2	rcp4.5 & rcp8.5
Atmosphere and Ocean Research Institute (The University of Tokyo), National Institute for Environmental Studies, and Japan Agency for Marine-Earth Science and Technology, **Japan**	MIROC	MIROC5	rcp4.5 & rcp8.5

Representative concentration pathways (RCP), is a greenhouse gas concentration (not emission), adopted by IPCC on its fifth Assessment Report in 2014 as the trajectory of climate change variables. It replaces Special Report on Emissions Scenarios (SRES) projections published in 2000. The possible carbon dioxide concentrations, warning and associated impacts of each RCP are summarized in the table below.

Table 4-2: RCP scenario and its expected impacts

Scenario	Atmospheric carbon dioxide concentrations in 2100 (used as input for most model simulations)	Temperature increase to 2081-2100 relative to a 1850-1900 baseline		Global mean sea level rise for 2081-2100 relative to a 1986-2005	
		Average	Likely range	Average	Likely range
RCP2.6	421ppm	1.6°C	0.9-2.3°C	0.40m	0.26-0.55m
RCP4.5	538ppm	2.4°C	1.7-3.2°C	0.47m	0.32-0.63m
RCP6.0	670ppm	2.8°C	2.0-3.7°C	0.48m	0.33-0.63m
RCP8.5	936ppm	4.3°C	3.2-5.4°C	0.63m	0.45-0.82m

Source: Department of Environment and Energy, Australian Government.

The following are figures showing climate change scenario based on RCPs from the past (historical) to future forecasted trend. The driving force of CO_2 concentration in particle per million (ppm), emissions (GtC) and global surface warning temperature (^0C) have shown below as follows:-

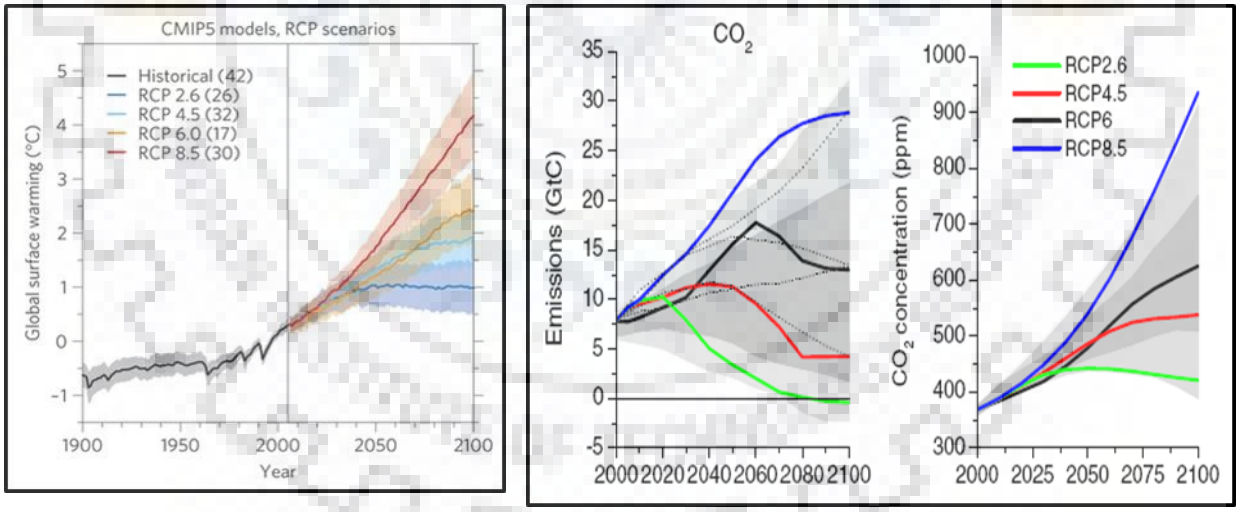

Figure 4.1: Forecasted RCP trend

4.3 Hydrological Model

4.3.1 Hydrological modeling for climate change impact studies

Hydrological model is a mathematical formulation, which estimates runoff response of watershed basin at the outlets from rainfall received by the basin. Todini et al., (2007) have stated that hydrological modeling range from the role of the physical based and data-driven model to concepts of predictive uncertainty and equifinality and their implications.

Changes in global climates have significant impacts on water resources. The impacts of the hydrological regime have modified the hydrological responses of some watershed, which have resulted in flow fluctuations. The hydrological regime impacts such as reduced streamflow have affected irrigation, water supply, aquatic ecosystem, and hydropower generation.

An evaluation of environmental change consequences for local water assets includes three stages, which incorporates (1) utilizing atmosphere model to recreate climatic impact of expanded atmospheric concentration of greenhouse gases (2) utilizing downscaling technique connecting climatic model and catchment-scale utilizing diverse climate scenarios and (3) utilizing hydrological model to simulate the effects of environmental change at catchment scale.

Most research conducted in many areas around the globe has shown that there is a significant change in the climate. The actuated environmental change on water assets needs more intervention in order to sustain water resources. The use of a hydrological model to assess annual and seasonal water availability play an imperative role in water assets management. The choice of model to use depend on many factors, which includes your objectives, applicability, and the complexity of the model and data availability. (Booij, 2004) Has analyzed the best way of model selection considering available data.

The reasons the HBV model is picked for this investigation is first since it is a proven model and has been being used for quite a while and it has likewise applied to numerous nations, for example, Zambia, Bolivia, Iran, Kenya, India, and others. However, has been applied to many basins and gave great outcomes in many applications Seibert, (2005), second, the model needs a moderate input data to generate/produce the yield of the model

With regards to the application, it requires just rainfall, temperature, and flows data which are promptly available to many countries. The input files are set up outside the HBV model with the specific format, catchment data files can be opened in the model subsequent to setting up all files. The client/user can specify catchment and model setting as well as parameter values to run the model simulation. In this model, there are two distinct tools available for automatic model calibration, Monte Carlo simulation and Genetic Algorithm and Powel optimization (GAP). The first can be used to run the large dataset with specified ranges of parameters with multiple catchments while the rest can run data set with single catchment with defined parameters. Results can be obtained in the resulting folder and different plot can be accessed based on your need as the researcher. In addition to that, also the user can specify areal distribution in a percentile according to arable land, forest, lakes or water bodies, and urban, etc. within the study area.

In this study, the catchment will be treated as a single catchment since the hydro met station is not evenly distributed. In addition to that, also there is no gauging data in some of the sub-catchment gauging stations. In the province of the investigation area, 15 hydro-met stations were considered for data analysis and evaluation. The HBV model will be applied with weighted temperature and rainfall obtained from the summation of multiplication of area ratio and temperature or rainfall. Discharge data is converted to depth in millimeter per day since the study area is known of about 67112.48 square kilometers by taking discharge divided to study area and multiplied by 1000 as a factor of changing meter cubic per second to a millimeter per day.

After preparing all files in the required format for the model for a run, this file will be opened HBV model and run the simulation. No matter if the result obtained for the first time is poor, calibration will be followed to improve results. In the calibration stage, the different parameter was changed and its output differences noted for sensitivity analysis check followed with the validation stage.

4.3.2 HBV Light model description

Hydrologiska Byrans Vattenbalansavdelning (HBV model is a semi-conveyed applied model of catchment hydrology which reenacts daily flows by utilizing daily temperature, precipitation, and estimated potential evaporation. The HBV model can be isolated into various vegetation and rise

zones just as into various sub-basins and sub-catchments. In this investigation, HBV Light Version 4.0.0.22 Seibert, (2009) is used for simulating stream and river flow. The main two contrasts between HBV Light and different renditions are in the model initialization, which ought to be finished utilizing warming up period in HBV Light, and a routing parameter that takes all real values instead of just integer values Seibert, (2005). The HBV model is a simple conceptual rainfall-runoff model, which is reasonable for various purposes, for example, the generation of long streamflow records, streamflow forecasting, and estimation of hydrological response of the watershed. It has been connected in a wide range of catchments, including the Rhine (the Linde et al., 2008; Hundecha and B'ardossy, 2004) and the Meuse (Leander and Buishand, 2007; Booij, 2005). As can be seen schematically in Figure 12 underneath, the HBV model

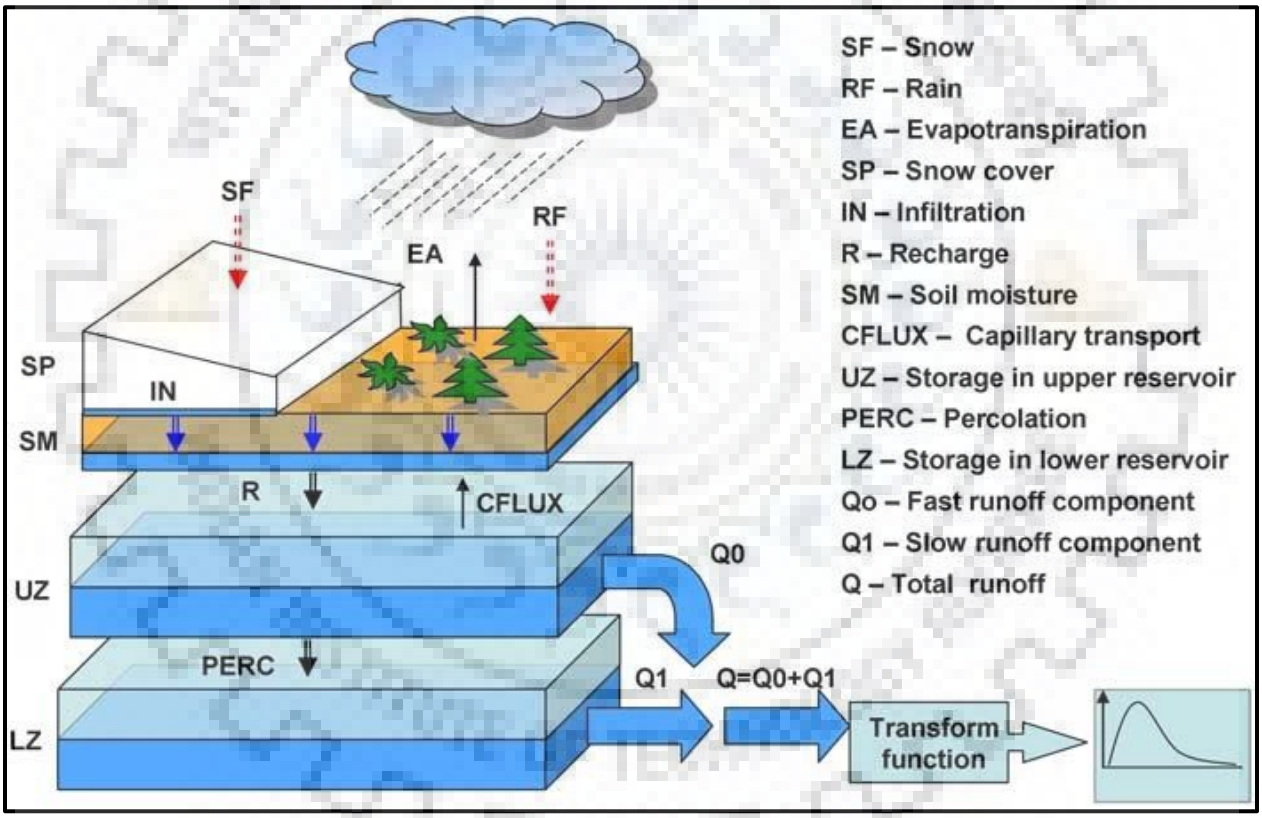

Figure 4.2: Schematic structure of the HBV model

depicts the water balance utilizing three storage reservoirs: a soil moisture zone, an upper zone storage (UZ) for sub-surface stormflow and a lower groundwater zone storage (LZ). Including an

algorithm for snow accumulation and melt (based on the degree-day method) and an algorithm accounting for lakes the general water balance equation becomes as follows:

$$P - E - Q = \frac{d}{dt}[SP + SM + UZ + LZ + lakes] \quad (4\text{-}4)$$

Where E, P, and Q allude to evaporation, rainfall, and runoff, respectively, all with measurements [L T^{-1}]. SP and SM represent snowpack and soil dampness, UZ, and LZ are identified with the upper and lower groundwater zone, all with measurements [L]. The lakes-term [L] refers to the capacity in lakes. The sub-zones for meteorological interpolation is available to represent the spatial distribution of temperature and rainfall. The model utilizes daily or hourly rainfall, temperature, and estimated potential evapotranspiration as input by Seibert, (2005)

HBV-light utilizes a warm-up period amid which state factors develop from standard introductory qualities to their proper qualities as per meteorological conditions and parameter values. One year of the warm-up is observed to be adequate much of the time. Rainfall is viewed as either snow or rain, contingent upon whether the temperature is above or beneath a threshold temperature, P_{TT} (^oC). All rainfall falling amid time steps when the temperature is beneath P_{TT}, i.e., reenacted to be snow and is multiplied by a snowfall adjustment factor, PSCF for redress blunder amid time step running the model. This factor adjusts for methodical mistakes in the snowfall estimations and for evaporation from the snowpack in the model, which isn't simulated expressly because of a tremendous error happening during the simulation. Snowmelt, M (mm/day), is determined with the degree-day technique utilizing the degree-day factor PCFMAX (mm/day/^oC). Meltwater and rainfall are held inside the snowpack until they surpass a specific fraction, PCWH, of the water equivalent of the snow. At the point when temperatures dip under P_{TT}, the measure of refreezing fluid water inside the snowpack, R (mm/day), is computed utilizing a refreezing coefficient, PCFR. In some catchment where it was applied, there is no snow and temperature does not go beyond the threshold, some of the parameters are non-sensitive.

4.3.3 Software functionality

HBV-light software adhering to a particular format, where catchment data can be opened in HBV light with various formats. In the utilization of this model, a client can specify data for catchment and the model, and the catchment settings just as parameter values to run the model recreation.

Results will be composed to yield records and, for the HBV-light GUI version, diagrams are produced in the outcomes. Other than running a solitary model reenactment, there are a couple of extra reproduction functional tools accessible. These tools are essential, highlights of the HBV-light software. Cluster simulated can be utilized to run the model for a rundown of predefined parameter sets. Moreover, there are two unique tools accessible for automatic model adjustments (calibration), Monte Carlo simulation and Genetic Algorithm and Powell optimization (GAP). Monte Carlo reenactments can be utilized to run a substantial number of simulations dependent on arbitrarily chosen parameter sets (inside client characterized parameter limits). Target capacities, for example, the Nash– Sutcliffe model effectiveness coefficient, are figured out for each model run and can be utilized to rank the diverse parameter sets dependent on their execution performance. The GAP calculation comprises of two stages (J. Seibert, 2012). First, improved parameter sets are created by a transformative mechanism of determination and recombination of a lot of introductory, arbitrarily chosen parameter sets (again inside client characterized parameter limits). Amid the second step, parameter sets can be tweaked utilizing Powell's quadratically convergent technique.

4.4 Method of downscaling and Tools

The General Circulation Models (GCM) used to reproduce the present and future climate utilizing main impetuses. The main impetuses of ozone-depleting substances, vaporizers and CO_2 concentration utilized for reenactment partition climate and sea into the flat network with the resolution of at least 1.90 to 3.750 latitude and longitude and with more than 12 to 30 layers in vertical. All in all, most GCM simulate continental and worldwide scale forms in detail and give a sensibly precise portrayal at a regional and worldwide scale. Trzaska, (2014) has expressed that, despite the fact that GCMs are important predictive tools, they are not able to account a fine heterogeneity of atmosphere inconstancy and change at high resolution. The various scene highlight, for example, mountain, infrastructure, land cover land use, and atmospheric climate component, for example, coastal breeze have a finer scale, which cannot be represented by more than 100-500 km spatial resolution.

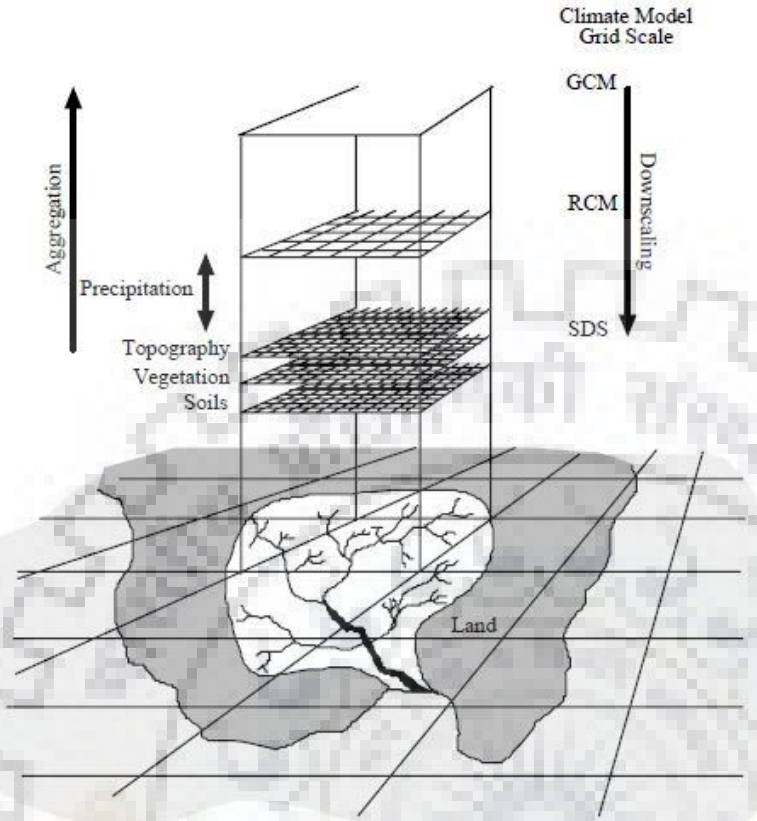

Figure 4.3: General approach schematic illustrating downscaling

(Sylwia Trzaska, 2014) Demonstrated the significance of downscaling since it is difficult to represent the local climate using GCMs. He has additionally, portrayed that it is vital to comprehend the downscaling procedure, of course, GCMs, with the goal that our fine yield is a pragmatist at a fine scale and capture well sub-grid heterogeneities

Dynamic and Statistical downscaling are only two methods generally available and utilized in climate change appraisal at local or station scale.

4.4.1 Dynamic downscaling

The dynamic downscaling method relies on the use of Limited-Area Model (LAM) or Regional Climate Model (RCMs). Principally RCMs are similar to GCMs but with higher resolution. The RCMs are nested to GCMs to capture the fine detail at a higher resolution. The output from RCMs still has a systematic error which often requires a bias correction and further downscaling to a finer

resolution. Kirtman, (2019) has stated that the RCMs cannot correct the profound error in large GCMs, therefore bias correction needed to improve the output representation.

4.4.2 Statistical (Empirical) downscaling

Statistical (Empirical) downscaling involves developing of the empirical relationship between large-scale climatic driving factors (predictors) and local surface variables (predictands). In most cases, predictions are observed/historical value in the field, which is used to estimate local climate using regional or global circulation models. Moreover, once the relationship has been determined and validated using historical data, the future local climate is predicted using calibrated and validated parameters to force GCMs for projection. The statistical downscaling focuses on single-site (point scale) summarized mathematically below as follows:-

$$L = F(G) \tag{4-5}$$

Where L speaks to the expectations (local climate variables), G speaks to the indicators (worldwide or territorial atmosphere expansive scale atmosphere factors) and F is deterministic/stochastic function conditioned by G and must be found exactly from the observed or modeled data set.

The advantage of using statistical downscaling method is computationally inexpensive which can be applied to many GCMs. In addition to that, also can provide site-specific information, which can be critically essential for most research on climate change issues to water resources. A diverse range of statistical downscaling techniques have been developed for many years and each method rely on three categories, namely stochastic weather generator, weather typing schemes, and regression (transfer function) method.

4.4.2.1 Stochastic weather generator

Weather generator (WGs) is a mathematical model, which generates synthesis weather series, which are statistically similar to local climate variables. The major statistical features such as average, variance, maximum/minimum, annual cycle, and correlations between variables are the same. It relies on statistics rather than the physical based mechanism used in GCM and RCM. Wilks, (2019) has stated that using weather generator provides a stochastic approach in downscaling where any combinations of small-scale (weather generator) conditions will be

consistent with any given large-scale. The Long Ashton Research Station Weather Generator (LARS-WG) is an example of stochastic downscaling used in climate change impacts studies.

4.4.2.2 Weather typing schemes

Weather typing schemes bunch days into a limited number of discrete climate type or "states" as indicated by their brief comparability. Cheng, (2011) has uncovered that brief weather typing schemes can characterize a complex set of meteorological variables.

4.4.2.3 Regression (Transfer Function) method.

Regression method downscaling relies on the quantitative relationship between local climate variables (predicted) and large-scale variables (predictors) which contain global climate information. Through some regression, the transfer function is developed between local climate variables and large-scale variables to establish the quantitative estimation of the local climate. It is revealed that multiple linear regression is specifically most accurate for estimate mean of local meteorological predictions by Pahlavan, (2018).

One of the most well known in statistical downscaling tools that implement regression is Statistical Down-Scaling Models (SDSM). SDSM version 4.2.9 facilitate the multiple regression development at low cost and at single site-specific. In addition to that, the software performs the ancillary task in data pre-processing such as quality data control, screening, transformation, and statistical analyses.

With regard to this research work, SDSM was selected to perform statistical downscaling by considering the following aspects

1) Model availability and its complexity in application
2) Downscaling to local climate and site-specific.
3) Data pre-processing and analysis

The SDSM software lessens the task of statistically downscaling daily climate series into seven discrete advances, for example, quality control and data transformation, screening of predictor variables, model calibration, weather generation (using observed predictors), statistical analyses graphing model output and scenario generation (using climate model predictors) as can be seen in figure 14 beneath.

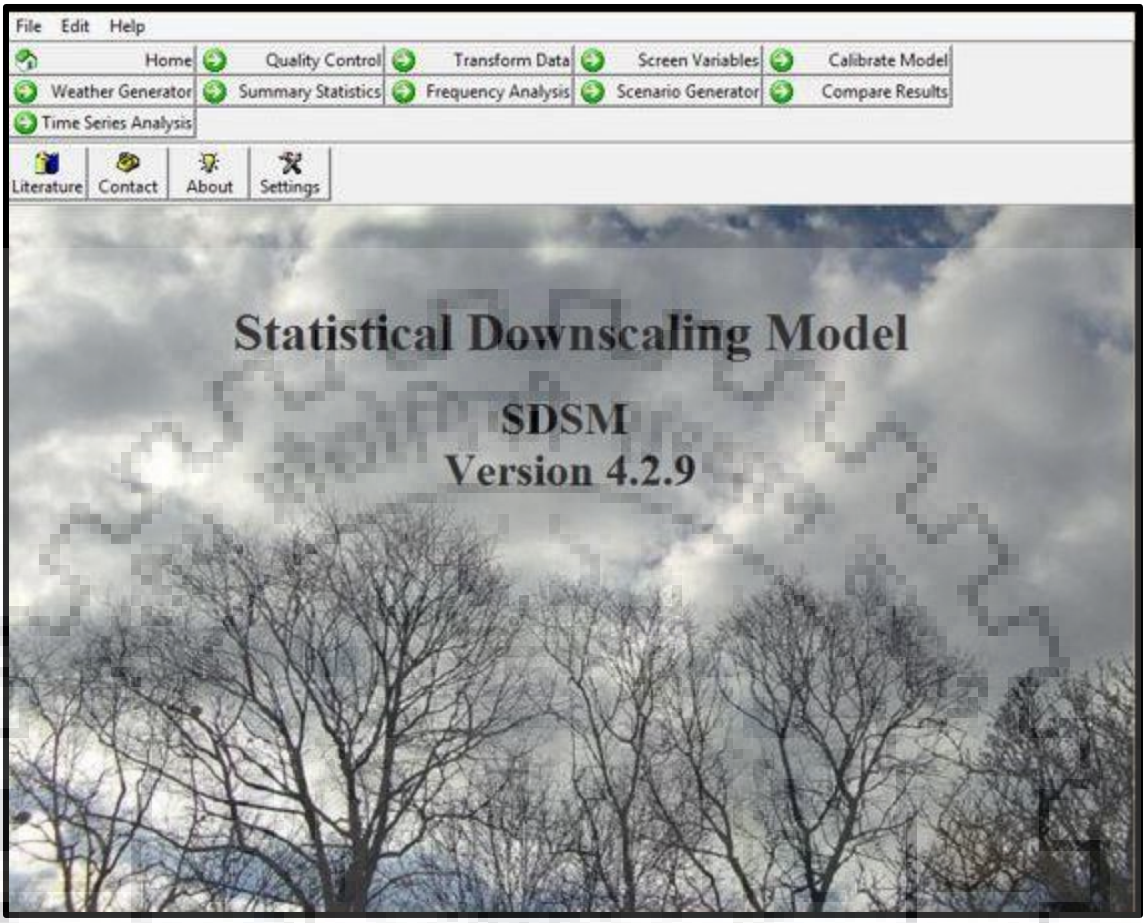

Figure 4.4: Main menu of SDSM 4.2.9

4.4.3 General Climate Model (GCM) grid for Statistical Downscaling Model (SDSM)

The study area was covered with 6 GCM raster nodes between latitudes 2^0 45′ and 5^0 42′ and longitudes 29^0 35′and, 33^0 40′ with a spatial resolution of 2^0 by 2.5^0. Only one GCM fall within the vicinity of the study area at the centroid of the catchment. The least GCM grid output resolution of 2^0 by 2.5^0 horizontal interval classified based on latitudes and longitudes. Due to the low spatial resolution of GCM, only one grid node used for downscaling. The combination of GCM raster nodes can be used if more than one nodes fall within the vicinity of the study area. It is difficult to consider nodes of the GCM that fall outside the study area due to uncertainty and low resolution associated with their locations. In many studies, they have highlighted ambiguities due to transposing of GCM from near area to your location of interest, which also attributes uncertainties during prediction. It is recommended to use the GCM which fall in the vicinity of the study area

for more accuracy and to be more precision when comes to capture the seasonality of the area of interest.

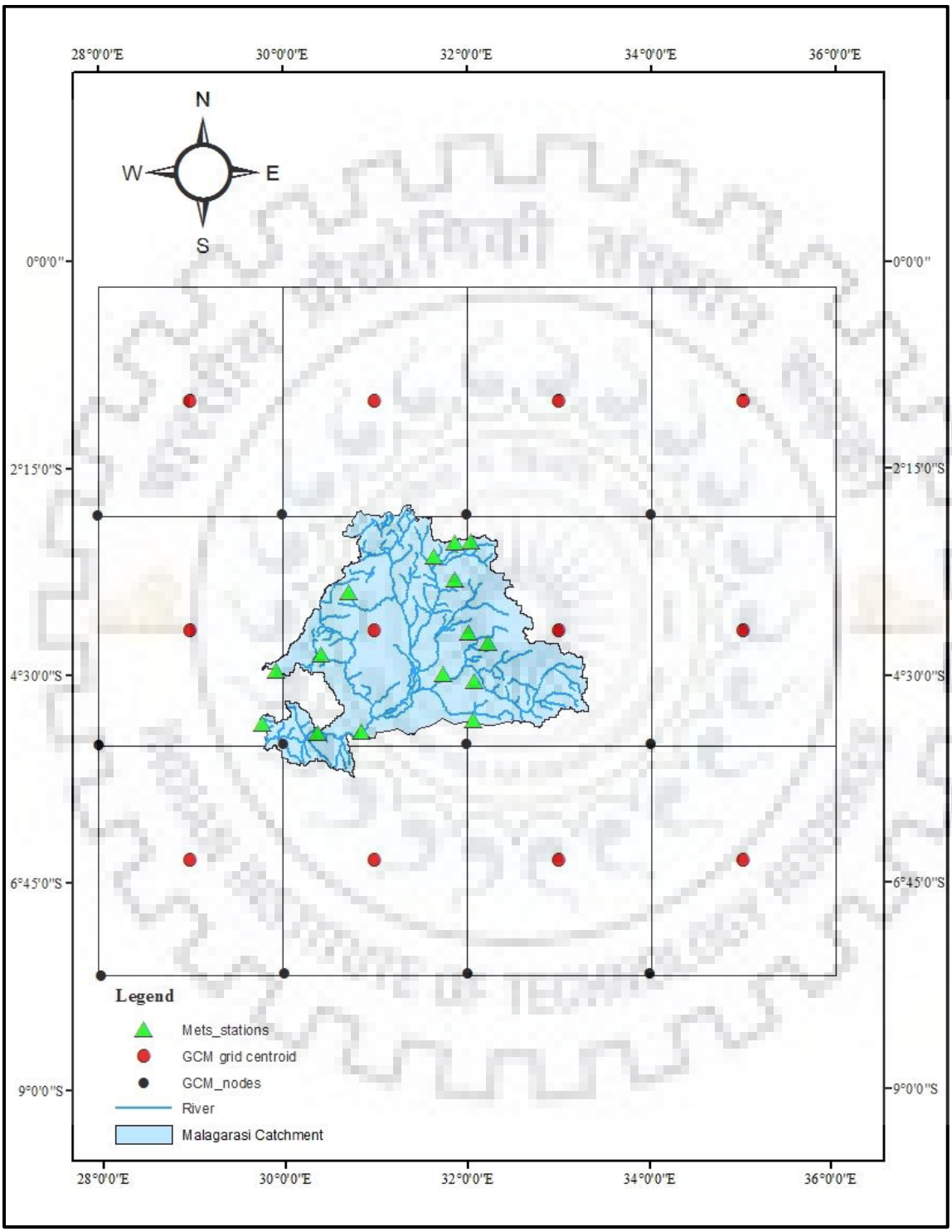

Figure 4.5: GCM grids selection in the study area

4.5 Methodology

4.5.1 Trend analysis and magnitude detection

This study work emphasizes determining the variation of temperature and rainfall over Malagarasi catchment. The presence of temperature and rainfall trends in the station data sets were tested using Mann-Kendall. The Thiel-Sen's estimator was used to estimate the magnitude of the trend. In many of the recent study test, statistics were checked at a 5% significance level.

4.5.1.1 Mann Kendall's test

Mann Kendall pattern test is valuable to identify a Monotonic pattern in time series. It can be utilized to check if there is any significant monotonic pattern in the time series. The Mann-Kendall test is a distribution-free, a non-parametric test for the pattern estimation of a time series. The MK test statistic is calculated as:-

$$S = \sum_{i=1}^{n-1} \sum_{j=i+1}^{j=n} sgn(xi - xj) \quad (4\text{-}6)$$

$$\text{sgn}(\theta) = \begin{cases} 1 \; if \; \theta > 0 \\ 0 \; if \; \theta = 0 \\ -1 \; if \; \theta < 0 \end{cases} \quad (4\text{-}7)$$

Mann- Kendall test without tie correction

For n ≥ 8, S is normally distributed as

$$E[S] = 0 \quad (4\text{-}8)$$

$$\text{Var(s)} = \frac{n(n-1)(2n+5)}{18} \quad (4\text{-}9)$$

Mann- Kendall test with tie correction:

$$E[S] = 0 \quad (4\text{-}10)$$

$$\text{Var(s)} = \frac{n(n-1)(2n+5)-\text{tc}}{18} \quad (4\text{-}11)$$

Tie correction

$$tc = \sum_{i=1}^{n} ti.i.(i-1)(2i+5) \quad (4\text{-}12)$$

Where: ti is the number of ties of degree i.

$$Zmk = \begin{cases} \frac{S+1}{(Var(S))^{\frac{1}{2}}} & S > 0 \\ 0 & S = 0 \\ \frac{S-1}{(Var(S))^{\frac{1}{2}}} & S < 0 \end{cases} \quad (4\text{-}13)$$

Z_{mk} is standard normally distributed with zero mean and unit variance

4.5.1.2 4.5.1.2 Theil-Sen median slope estimator

It is utilized to estimate the true slant of an existing pattern as a change per time step, the Theil-Sen slope estimator nonparametric method is mostly utilized in the determination of the magnitude of the trend. This method can be used for the case when the pattern is thought to be linear. This equation can be written as

$$h(t) = Qt + C; \quad (4\text{-}14)$$

where Q is the median slope and C is a constant

To get the slope estimate Q in the equation we first compute the slope of all fatal value pairs in the data set as defined as in equation

$$Q_i = \frac{xj - xk}{j - k} \quad (4\text{-}15)$$

Where j >k

In the event that there are n esteems x_j in the time series, we get the same number of as

$$N = n(n-1)/2 \quad (4\text{-}16)$$

From eqn 18, Qi estimated by slopes. The Theil-Sen's estimator of the incline is the median of these N estimations of Qi. The N estimations of Qi are arranged from the smallest to the largest and estimated as beneath

$$Q = Q_{[(N+1)/2],} \text{ if } N \text{ is odd} \quad (4\text{-}17)$$

$$Q = \frac{1}{2}\left(Q_{[N/2]} + Q_{[(N+2)/2]}\right), \text{ if } N \text{ is even} \quad (4\text{-}18)$$

In addition, the percentage of change of the magnitude of the entire period was calculated by using the formula below.

$$\%\text{ of change of the magnitude} = \frac{\text{median slope} * \text{length period of} * 100\%}{\text{Mean}} \quad (4\text{-}19)$$

CHAPTER FIVE: RESULT AND DISCUSSION

5.1 Trend analysis and Magnitude

Different stations were selected from the study area for analysis, especially stations with at least complete data. The trend analysis was performed using Man-Kendall test and magnitude were performed using Thiel-Sen slope estimator

5.1.1 Temperature

In the analysis of temperature, the heterogeneous trends were noted from different GCM. The magnitude revealed inconsistence trend in some of the forecasted data from GCM output. The following were the results tabulated in Table 5-1 below

Table 5-1: trend analysis and magnitude values

Observed Temperature (1983-2015)		
Stns ID	Trend	Magnitude
9231005	0.324	0.035
9231016	-0.0045	-0.004
9330000	0.678	0.049
9330005	1.024	0.324
9330006	1.654	0.412
9330007	0.0023	0.002
9331001	0.039	0.007
9332001	0.075	0.34
9430002	1.083	0.271
9430005	-0.041	-0.024
9431000	0.035	0.034

Forecasted Temperature							
GCM	Scenario	Trend Period			Magnitude period (%)		
		2030s	2050s	2080s	2030s	2050s	2080s
MIROC	RCP4.5	-0.84	-1.68	-0.87	-3.4	-9.2	-4.8
	RCP8.5	-0.75	-0.57	-0.07	-2.6	-3.1	-1.2
BNU	RCP4.5	-0.93	0.14	-0.72	-2.7	1.9	-2.1
	RCP8.5	-0.97	-1.89	-1.27	-3.3	-4.2	-6.2
CanESM2	RCP4.5	0.04	1.25	1.51	0.98	10.4	9.2
	RCP8.5	1.41	-0.82	-0.17	12.3	-3.9	-4.7
CSM1.1	RCP4.5	-1.10	0.25	0.47	-1.3	6.4	8.9
	RCP8.5	0.00	1.46	**2.16**	0.1	9.7	12.9

More than 80% of the historical data stations collected from the representative stations have shown that there is an increase in temperature trend from 1983 to 2015 of the analysis period. However, the forecasted temperature have shown the heterogeneous trends, where for MIROC have revealed that they will be the decrease of temperature for all near future, middle future and late future horizon ranging from 1.2% to 9.2%. Moreover, BNU showed that there would be a decrease in

temperature of 2.1% and 6.2% for near and late future horizon respectively while an increase of 1.9% for the mid future. In addition to that, CanESM2 have shown an increase in temperature for all future skyline at RCP 4.5 of 0.98%, 10.4% 9.2% respectively. While for Can ESM2 RCP 8.5 showed an increase in temperature of 12.3% for the near future and a decrease of temperature for the middle and late future skyline of 3.9% and 4.7% respectively. The CSM1.1 also showed that only decrease of temperature for RCP4.5 in the near future of about 1.3% and an increase of temperature for middle and late future for RCP 4.5 and RCP 8.5 ranging from 0.1% to 12.9%. In the near future of CanESM2, RCP 8.5 has shown no trend.

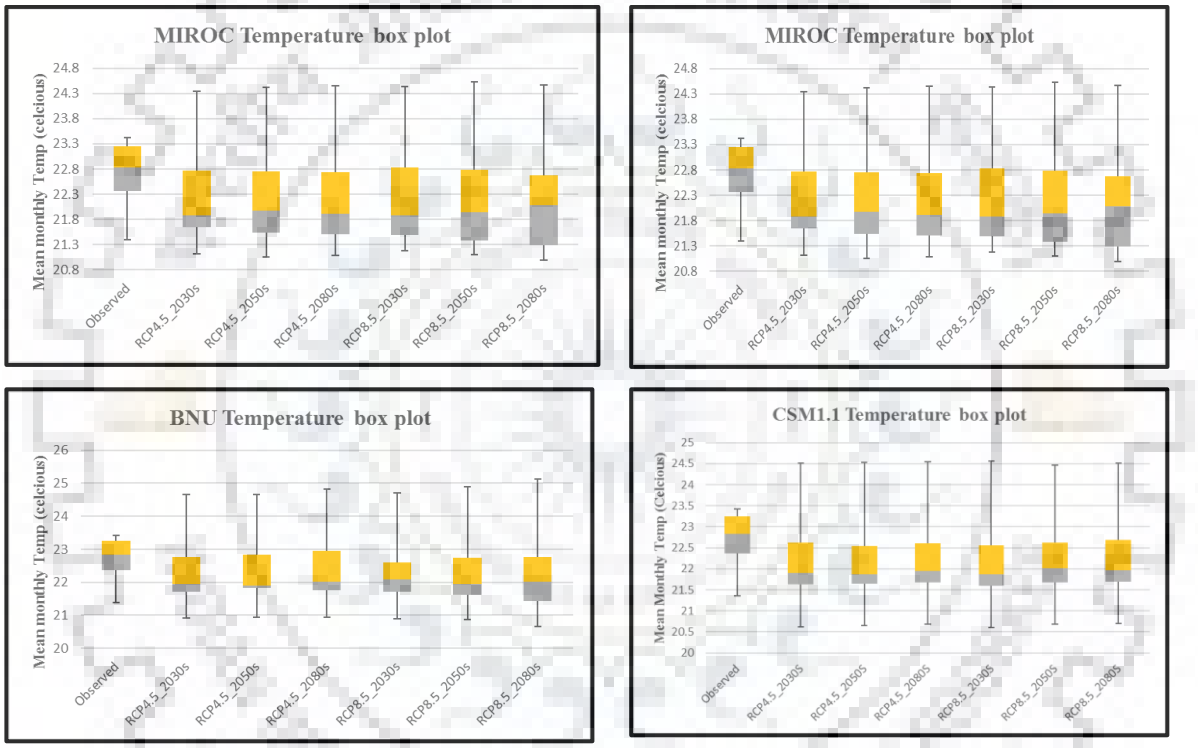

Figure 5.1: Forecasted GCMs Temperature box plots

The most of forecasted temperature depicts declining trend which is insignificant at 5% significance level, except for CSM1.1 GCM of the period spinning from 2075-2100 (the 2080s) shown increasing trend significant at 5% significance level with a trend of 2.16. Although IPCC suggests that East Africa will experience a warming of 0.3^0C to 1.0^0C at the end of the 21st century, most of the forecasted temperatures from different GCM have shown a decline. This may be attributed to localized climate and uncertainty during downscaling and projection. It must be noted that is possible for GCM to project global or continent temperature correctly compared to the station or local scale.

5.1.2 Rainfall

More than 17 meteorological stations were selected for analysis in the study area. However, 47% of the selected rainfall stations have shown the decrease of rainfall while the rest showing the insignificant increase of the rainfall ranging from 0.7% to 2.4%. The following are the analysis results tabulated in table 5-2 below.

Table 5-2: Rainfall trend analysis and Magnitude

Observed Rainfall (1983-2015)		
Stns ID	Trend	Magnitude
9231005	-0.448	-1.004
9231006	0.169	0.083
9231016	-1.025	-2.690
9330000	1.886	0.010
9330002	0.433	0.753
9330005	-3.093	-1.130
9330006	-3.074	-0.976
9330007	0.754	0.031
9331001	1.028	0.950
9331004	-2.097	-0.323
9332001	1.073	0.530
9429000	-0.056	-0.003
9430002	-0.076	-0.041
9430005	1.094	0.320
9431000	0.453	0.021
9431001	0.567	0.067
9529002	-1.035	-0.870

Forecasted Rainfall							
GCM	Scenario	Trend Period			Magnitude period (%)		
		2030s	2050s	2080s	2030s	2050s	2080s
MIROC	RCP4.5	-0.40	-1.21	**2.06**	-0.5	-3.4	1.2
	RCP8.5	-0.97	-0.57	-0.02	-3.4	-0.7	-1.7
BNU	RCP4.5	0.75	-0.32	0.12	2.1	-0.3	4.7
	RCP8.5	2.03	-0.86	0.07	1.4	-0.9	0.3
CanESM2	RCP4.5	-1.23	0.50	**2.60**	-0.9	1.3	2.2
	RCP8.5	-1.41	-0.89	-1.41	-3.1	-0.2	-0.3
CSM1.1	RCP4.5	-1.15	0.93	-2.55	-3.7	0.6	-0.2
	RCP8.5	0.57	-0.25	**2.16**	2.3	-1.3	5.9

The forecasted rainfall has revealed that expected rainfall is going to lessen in more often than not, a vast majority of the GCM showed. However, MIROC has demonstrated the decline of rainfall in all scenarios running from 0.5% to 3.4% except the scenario of RCP4.5 in the late future, which demonstrated an expansion of rainfall of about 1.2%. Nevertheless, BNU has demonstrated an increase of rainfall for all near and late future horizon extending from 0.3% to 4.7 % in all scenarios, only demonstrated an increment of rainfall in the middle future of 0.3% to 0.9% for all scenarios. The CanESM2 GCM have demonstrated a reduction of rainfall for scenario RCP8.5 running from 0.2% to 3.1%, and for the scenario, RCP4.5 diminishing of rainfall of about 0.9% in

the near future and expansion of rainfall for middle and late future of 1.3% to 2.2% respectively. Moreover, CSM1.1 demonstrated a lessening of rainfall for RCP4.5 in the near and late future timeline of about 3.7% and 0.2% respectively, while there would be an expansion of rainfall in the middle future (the 2050s) of 0.6%. With respect to RCP 8.5, CSM1.1 have demonstrated a lessening of about 1.3% in the middle future and expansion of rainfall in the near and late future 2.3% and 5.9% respectively.

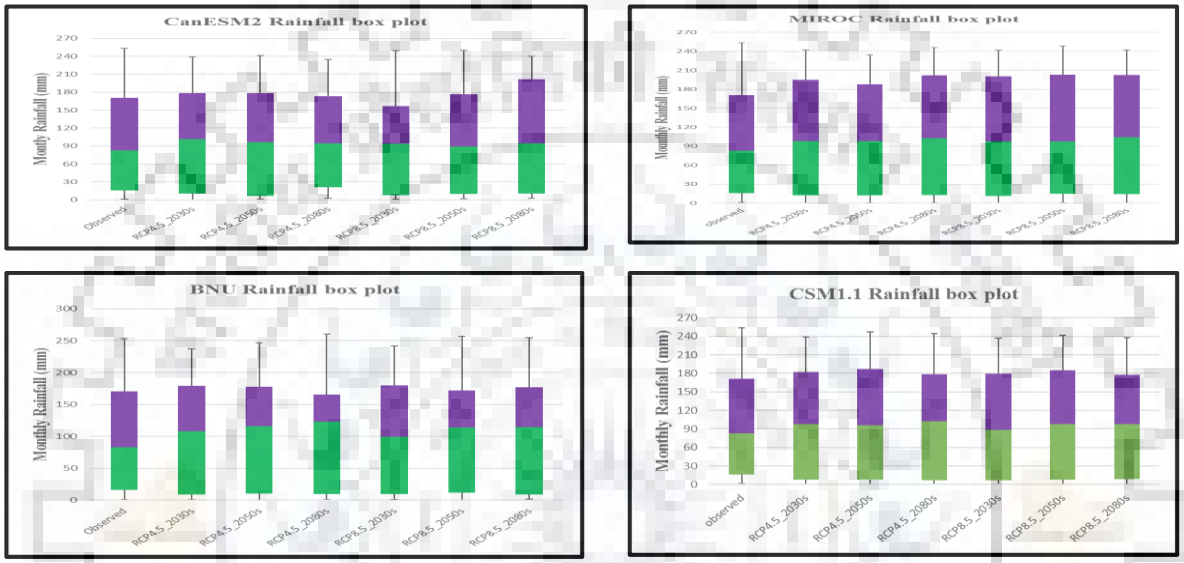

Figure 5.2: Forecasted GCMs Rainfall box plots

The observed historical rainfall showed no clear trend insignificant at 5% significance level while the forecasted rainfall showed a declining trend in most GCMs except late future (2080s) timeline of MIROC RCP4.5, CanESM2 RCP4.5, and CSM1.1 RCP8.5. These showed increasing trends significant at 5% significant level with the trend of 2.06, 2.60, and 2.16 respectively as can be shown in table 5.2 above. In addition, the box plot in figure 5.2 has demonstrated the same correspondence of the yearly observed and forecasted rainfall.

5.1.3 Discharge

Discharge measurements at the outlet of the catchment have expressed from 1977 till to date, yet there is a missing hole in certain periods. The authentic estimations taken regularly have demonstrated a decline in pattern from 1977 to 2015 of the examination time frame. The chronicled information dissected from 1977 to 2015 has appeared immaterial lessening in the pattern at 5% noteworthy dimension of the extent of 4.6% per annually.

5.2 The calibration and validation results of hydrological model

The modification is done physically by upgrading the model parameters in each subroutine that fundamentally influence the execution of the model. In light of this, few runs made to pick the best parameter set, which coordinates the observed discharge with the simulated discharge in which ten years data were utilized for adjustment and five years data for approval. The outcomes of each run were assessed by considering various criteria as mentioned below;

1. Comparison between the estimated and observed hydrograph and visual inspections.
2. Nash Sutcliffe Efficiency criteria (NSE).
3. Coefficient of assurance (R^2)

The following are the most optimal parameter set used in this research summarized in table 7, which categorized as follows;

Table 5-3: Model estimated parameters

Parameter	Explanation	Minimum	Maximum	Value obtained
Snow routine				
TT	Threshold Temperature	-1.5	2.5	1.2
CFMAX	Degree-day factor	1	10	3.45
SCF	Snow Correction Factor	0.4	1	0.7
CWH	Water holding capacity	0	0.2	0.1
CFR	Refreezing coefficient	0	0.1	0.05
Soil routine				
FC	Maximum of SM (storage in soil box) (mm)	50	5000	4000
LP	Threshold for reduction of evaporation (SM/FC)	0.3	1	0.4
BETA	Shape coefficient	1	6	3.7
CET	Correction factor for potential evaporation	0	0.3	0.04
Response routine				
K1	Recession coefficient (upper box) (d^{-1})	0.01	0.4	0.01
K2	Recession coefficient (lower box) (d^{-1})	0.001	0.15	0.02
PERC	Maximum flow upper to lower box (mmd^{-1})	0	3	0.2
MAXBAS	Routing length of weighting function (d)	1	7	1

The observed and simulated hydrograph utilizing the above ideal parameters are shown in figures 5.3 below. Visual examination of the watched and recreated hydrograph exhibits that the execution of the model in forecasting the base flow, rising and subsidence appendage of the hydrograph is great. The high flows model simulation is palatable in spite of the underestimation of high single peaks in 2004. The objective function utilized for assessment shown execution as demonstrated before in section 4.2.1, the fundamental model performance indicator of Nash-Sutcliffe Efficient (NSE) in HBV light model demonstrated an equivalent to 85.43% during adjustment stage. In general, execution of the model as far as reproducing the observed hydrograph can be viewed as palatable for the particular motivation behind this scope.

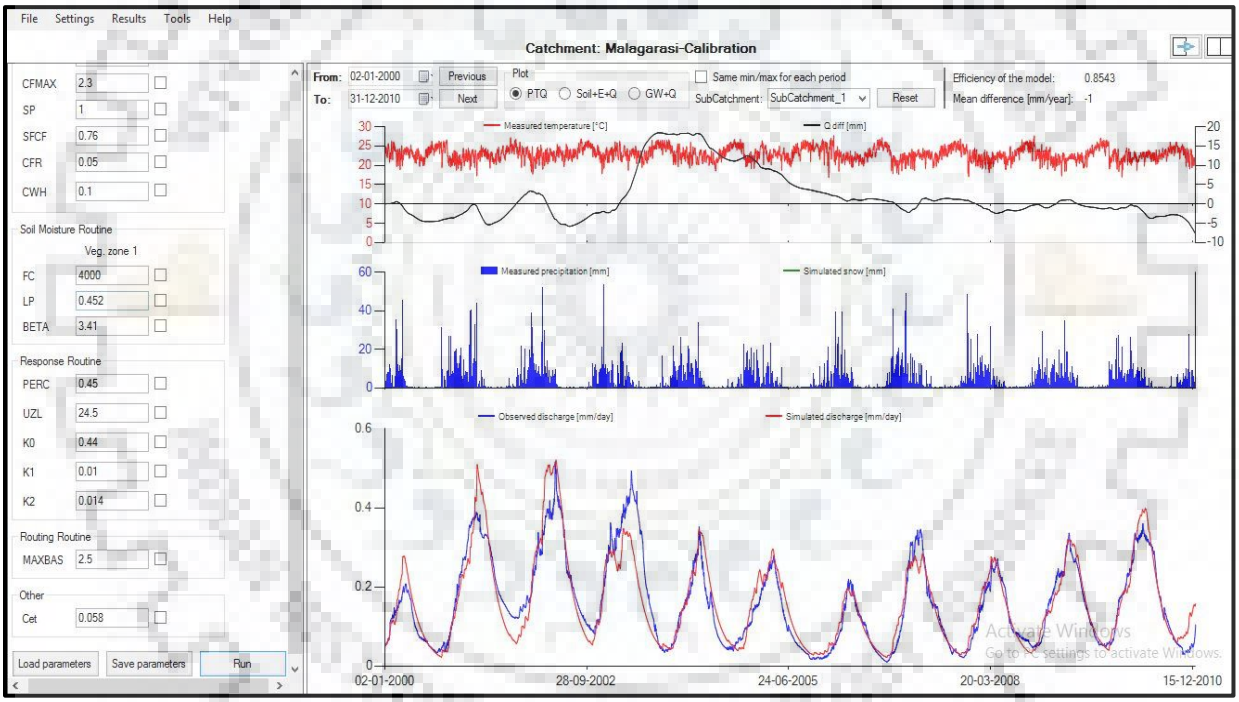

Figure 5.3: Model calibration

The model outcomes summary statistics additionally displayed in underneath figure 5.4 below. The model summarized well the statistical performance criterion considered amid the execution. Although visual inspection was considered regardless, whether the statistical parameter is by all accounts agreeable.

Malagarasi-Calibration

Water Balance [mm/year]		Subcatchment 1
Sum Qsim	=	59
Sum Qobs	=	58
Sum Precipitation	=	985
Sum AET	=	932
Sum PET	=	1002
Contribution of Q0	=	0.000
Contribution of Q1	=	0.042
Contribution of Q2	=	0.958

Goodness of fit		
Coefficient of determination	:	0.8620
Model efficiency	:	0.8543
Efficiency for log(Q)	:	0.8711
Flow weighted efficiency	:	0.8300
Mean difference	:	-1
Efficiency for specified season	:	0.8543

Figure 5.4: Model results summary during the calibration period

The model additionally approved utilizing the autonomous set data that not utilized amid the adjustment period by a similar parameter set. The simulation of discharge during the approval stage was great and the model efficiency Nash Sutcliffe Efficiency (NSE) and coefficient of assurance (R^2) of 85.77% and 85.95% respectively considered satisfactory. Figure 5.5 underneath demonstrate the match correspondence to simulated and observed hydrograph amid the approval period.

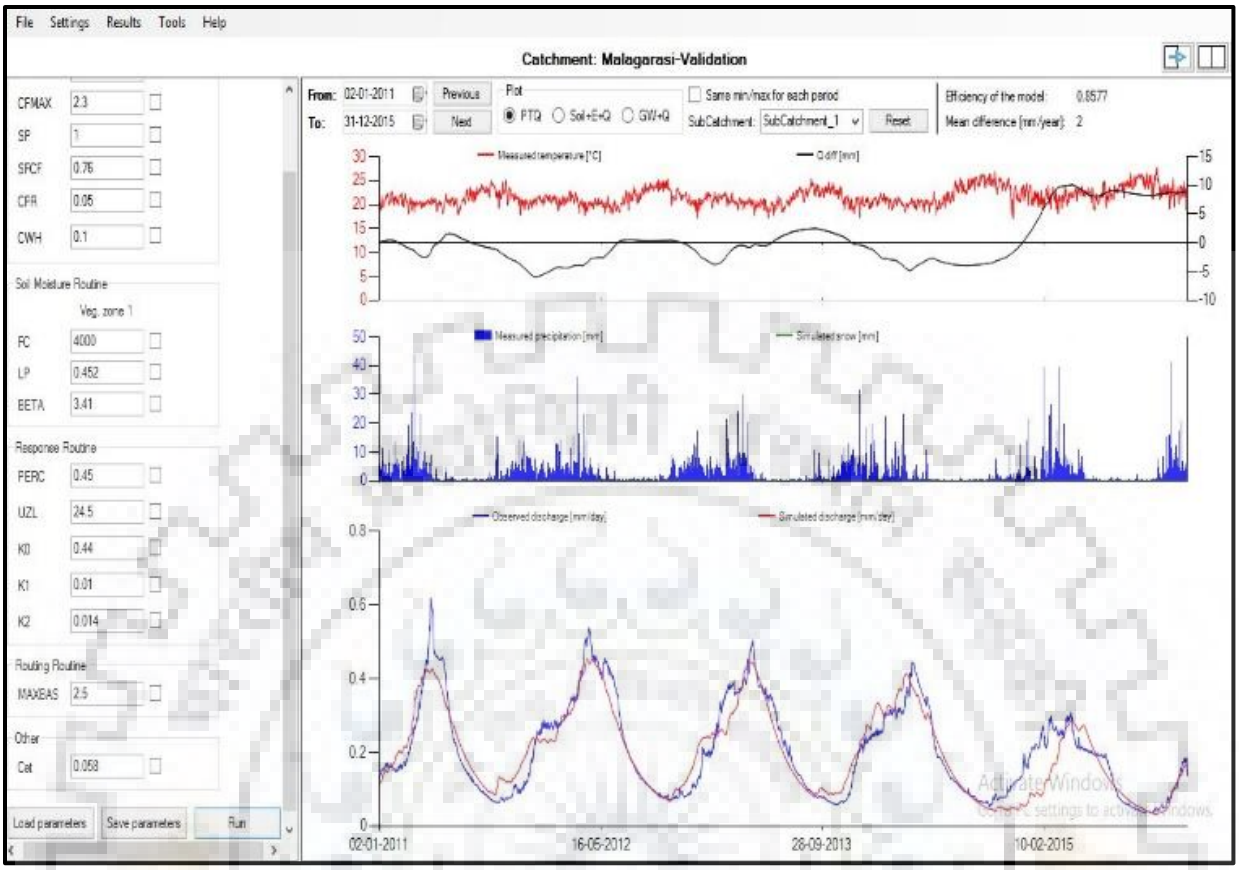

Figure 5.5: Model calibration

In addition, their corresponding statistics from the model analysis were presented in figure 5.6 below. The model summarized qualitatively and quantitatively well in performance during the validation period.

Malagarasi-Validation

Water Balance [mm/year]		Subcatchment 1
Sum Qsim	=	73
Sum Qobs	=	75
Sum Precipitation	=	954
Sum AET	=	906
Sum PET	=	930
Contribution of Q0	=	0.000
Contribution of Q1	=	0.044
Contribution of Q2	=	0.956

Goodness of fit		
Coefficient of determination	:	0.8593
Model efficiency	:	0.8577
Efficiency for log(Q)	:	0.7940
Flow weighted efficiency	:	0.8674
Mean difference	:	2
Efficiency for specified season	:	0.8577

Figure 5.6: Model results summary during the validation period

5.3 Hydrological Modeling for future climate impacts

To understand future discharge pattern, the examination was done occasionally from January to December. All GCM have demonstrated a reduction in discharge for the months from January to June and marginally increment of flows for the time of July to the center of October. The exceptional increment of release was noted for the period beginning from the finish of October to December. The summary of forecasted discharge from different GCMs condensed in figure 5.7, 5.8, 5.9, and 5.10 below.

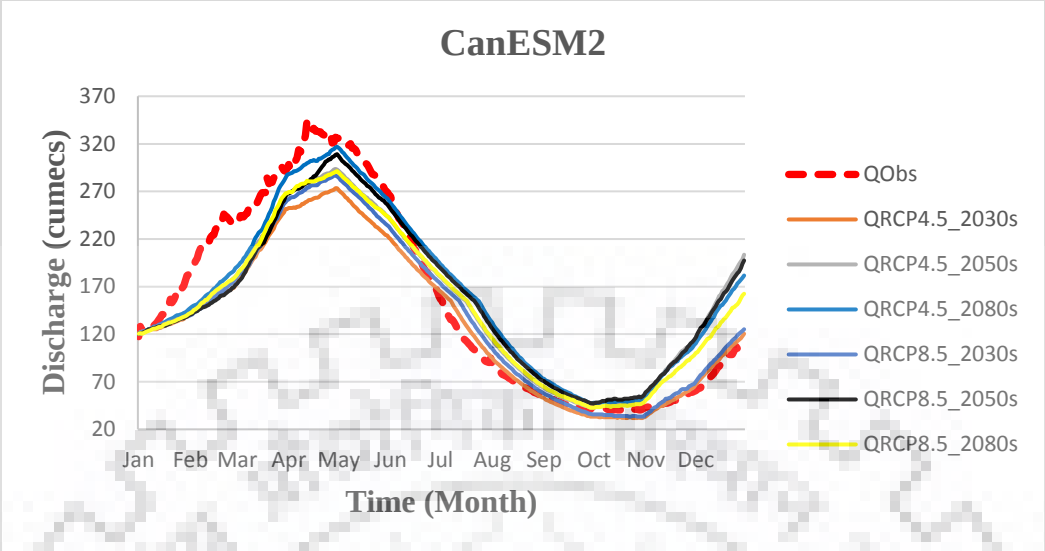

Figure 5.7: forecasted discharge using CanESM2 GCM

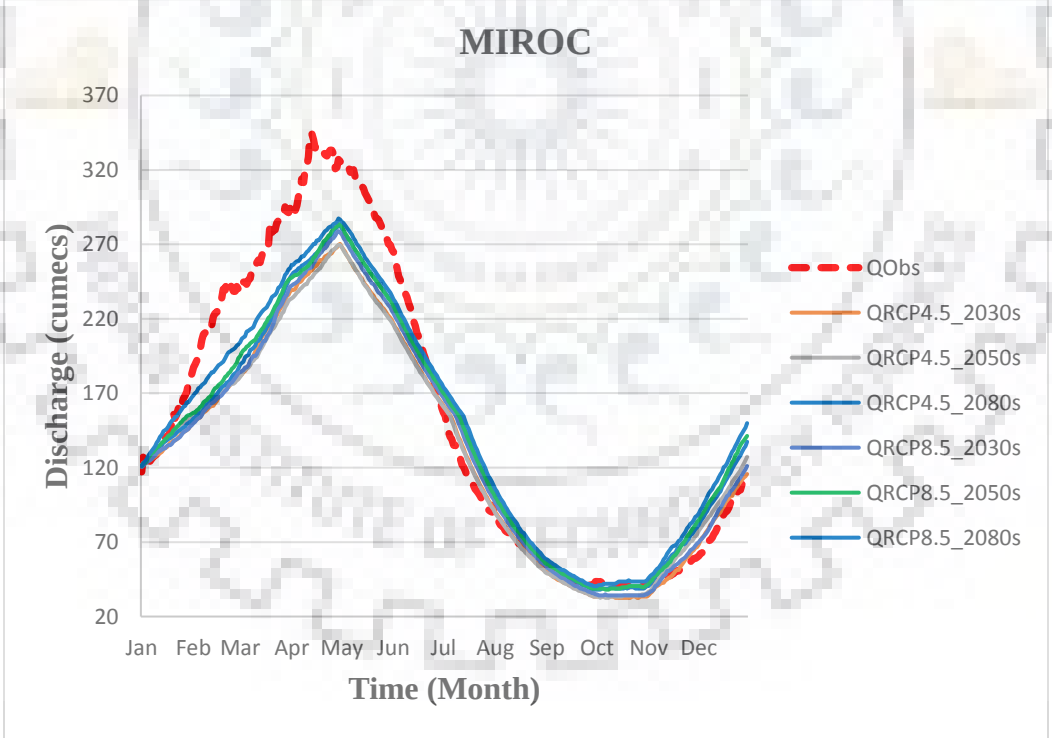

Figure 5.8: forecasted discharge using MIROC GCM

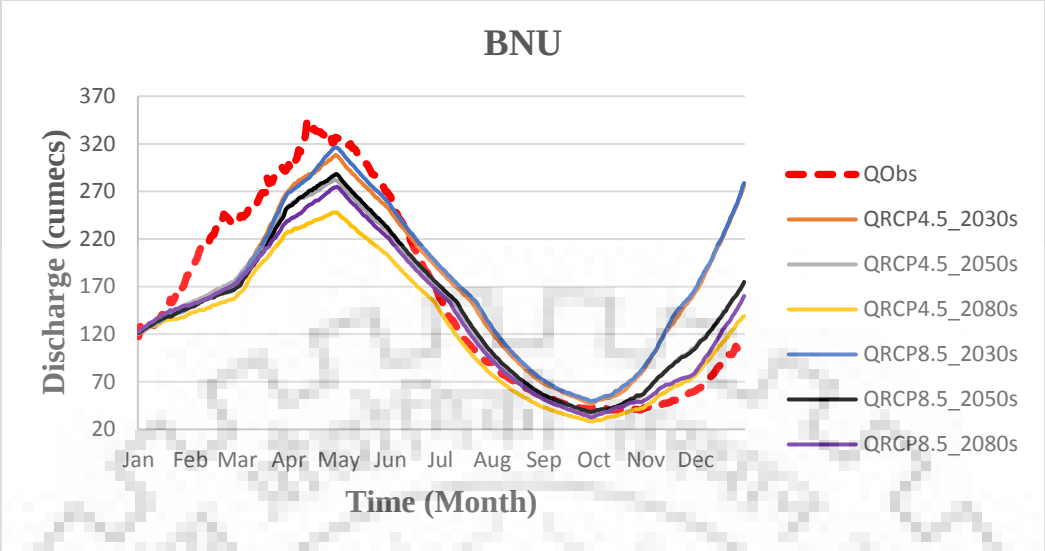

Figure 5.9: forecasted discharge using BNU GCM

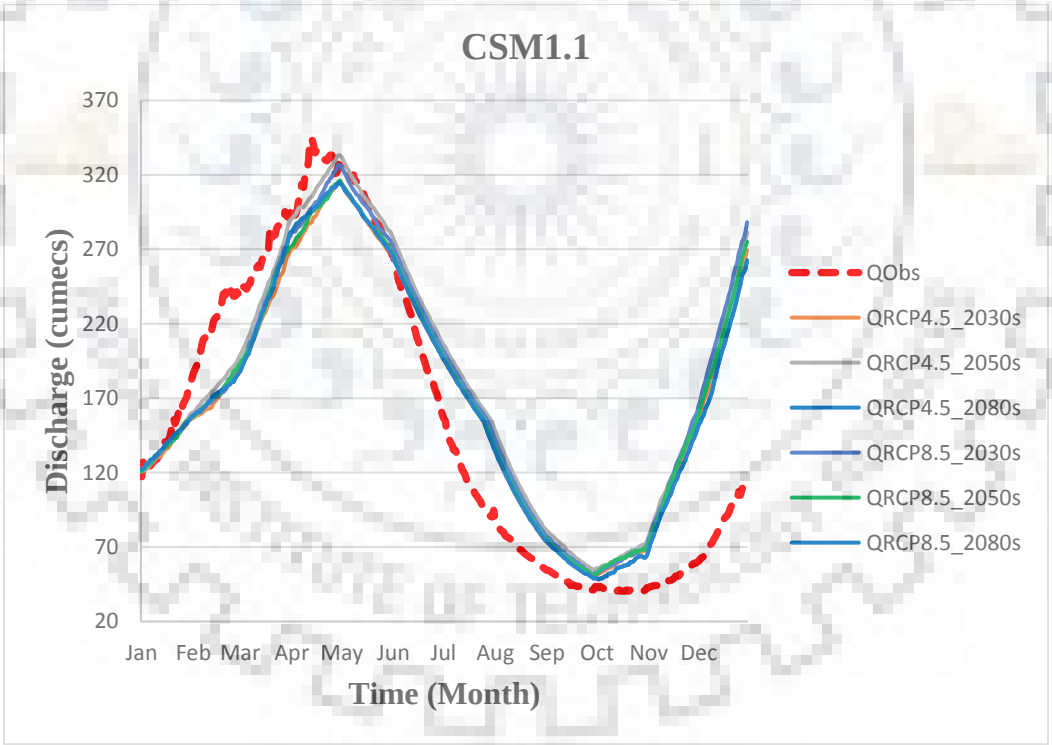

Figure 5.10: forecasted discharge using CSM1.1 GCM

Table 5-4: GCM discharge statistics summary

GCM		QObs	QRCP4.5			QRCP8.5		
			2030s	2050s	2080s	2030s	2050s	2080s
MIROC	sum	56888.70	48683.73	49000.65	51862.26	49851.21	52223.45	54389.07
	Diff		-8204.97	-7888.05	-5026.45	-7037.49	-4665.25	-2499.63
	%		**-14.42**	**-13.87**	**-8.84**	**-12.37**	**-8.20**	**-4.39**
CanESM2	sum	56888.70	49043.38	56201.26	59260.16	51376.78	57550.51	55062.53
	Diff		-7845.32	-687.44	2371.46	-5511.92	661.80	-1826.17
	%		**-13.79**	**-1.21**	**4.17**	**-9.69**	**1.16**	**-3.21**
BNU	sum	56888.70	61007.11	53160.23	45981.37	61940.00	53306.26	50530.10
	Diff		4118.41	-3728.47	-10907.33	5051.30	-3582.44	-6358.60
	%		**7.24**	**-6.55**	**-19.17**	**8.88**	**-6.30**	**-11.18**
CSM1.1	sum	56888.70	62578.50	65953.55	62496.94	64550.71	63306.33	62496.94
	Diff		5689.80	9064.85	5608.24	7662.01	6417.63	5608.24
	%		**10.00**	**15.93**	**9.86**	**13.47**	**11.28**	**9.86**

As can be seen in the table above, all GCM have shown a decrease of runoff at the outlet except CSM1.1, which showed an increase. With respect to MIROC GCM, have shown a decrease of runoff at the outlet ranging from 8.84% to 14.42% and 4.40% to 12.40% for scenario RCP4.5 and RCP8.5 respectively. Moreover, CanESM2 depicted decrease of runoff of 13.79% and 1.21% for period 2030s and 2050s respectively of RCP4.5 while an increase was noted in the late future horizon (2080s) of about 4.17%. For the scenario, RCP8.5 of CanESM2, have shown a decrease of runoff in the near (the 2030s) and late (2080s) future horizon of about 9.69% and 3.21% respectively and an increase of 1.16% in the middle future (2050s). However, BNU showed an increase of runoff in the near future for all scenario RCP4.5 and RCP8.5 of 7.24% and 8.88% respectively. The decrease was noted in the middle (2050) and late (2080) future horizon of 6.55% and 19.17% for RCP4.5 and 6.30% and 11.18% for RCP8.5 respectively. CSM1.1 have shown an increase of runoff at the outlet for all scenarios of RCP4.5 and RCP8.5 ranging from 9.86% to 15.93% respectively.

As summarized in table 5.4, it is expected that there will be a decrease of discharge at the outlet of the catchment as were shown by most GCMs. The more alteration of discharge is expected during high flows (wet season). In the wet season, they will be a significant decrease of flows ranging from 6.68% to 21.18% which could directly affect socio-economic activities such as irrigation, hydropower generation, and water supply.

CHAPTER SIX: CONCLUSIONS AND LIMITATIONS

Water plays a significant role in the society and nature underscore the need for comprehension of how the change in worldwide atmosphere could influence the accessibility and dependability of water assets at a catchment scale. However, this is convoluted by the way that the environmental change data required for effects contemplates is of a spatial scale much finer than that given by the General Circulation Model (GCM). The existing mismatch between the two processes is somewhat settled by a vulnerability. The issue was exacerbated by the absence of good quality information for a fundamentally extensive stretch of the study area. In spite of this, the maximum effort was made to research the possible fate of hydrological effects of climate change and coming up next are conclusion and limitations in this examination.

6.1 Conclusions

- From the outcomes connected to the statistical downscaling model, demonstrate that they are decreasing trend pattern in mean annual temperature in the future timeline for both RCP4.5 and RCP8.5 scenarios. The mean annual temperature will decline by 0.3^0C and 0.5^0C for RCP4.5 and RCP8.5 scenarios respectively at the end of the 21st century. Climate change scenario for Africa from several General Circulation Model (GCM) utilizing the information gathered by the Intergovernmental Panel on Climate change Data Distribution Center (IPCC-DDC) demonstrated warming crosswise over Africa in the future with a range from 2^0C (low scenario) to 3^0C (worst scenario) by the end of 2100. Meanwhile, the estimated temperature warming range for East Africa ranges from 0.5^0C to 1.0^0C according to the Climate and Development Knowledge Network report of 2014, after the revision of the IPCC fifth assessment report. Hence, the outcomes analyzed and obtained from SDSM fail to fall in IPCC suggestions. Hence, may be attributed by uncertainty during downscaling and projection, but provide insight on how the future could behave. Further study is emphasized to check the contrast of my result and IPCC suggestions

- The rainfall downscaling consequences are that the rainfall does not show a deliberate increment or lessening in all future time skyline for both RCP4.5 and RCP8.5 scenarios not at all like that of temperature. However, 70-80% of yearly rainfall of the study area is

concentrated in four months of January, February, March, and April with marginal rainfall in April. The mean month to month rainfall shows an expansion pattern in the start of the rainy season (October to December) and diminishing pattern towards the finish of the rainy season (February to April) for both RCP4.5 and RCP8.5 scenario in all future timelines. Somewhat expansion was seen in July to September for both rcp4.5 and rcp8.5 scenarios in all future time horizon by 2.5% and 4.7% respectively. The downscaled rainfall catch well the seasonality of the study area, where the maximum and minimum rainfall is relied upon to be in April and October respectively, which match with the current local climate.

- The aftereffect of HBV in hydrological model calibration and validation demonstrates that the simulation of runoff was considerably good. The model performance criterion, which is utilized to assess the model outcomes, shows Nash-Sutcliffe Efficient (NSE) criteria are 85.43% and 85.77% during calibration and validation period respectively. However, the coefficient of determination R^2 of over 86% was obtained in all cases.

- The hydrological impacts of climate change scenario showed that there an exceptionally occasional and monthly variety of runoff contrasted with the yearly variety. In the fundamental rainy season (February to April), the runoff will be diminished by the average of 6.7% and 11.3% for RCP4.5 and RCP 8.5 respectively for all future time horizon. The mean yearly runoff will lessen by 14.42% and 12.37% for RCP4.5 and RCP8.5 scenario respectively within a similar period.

- Evaluation of climate change is extremely important to adapt to consistently evolving conditions. The pattern examination is made for Malagarasi catchment for annual rainfall data for period 1977-2015 is performed utilizing a non-parametric Mann-Kendall and Sein slope Estimator test. The outcomes uncover a descending pattern for most of the year for the period under scrutiny. Since months of substantial rainfall including 70-80% of the complete yearly rainfall, i.e. January-April demonstrates a noteworthy diminishing pattern, it tends to be surmised for the seasonal (wet season) rainfall over Malagarasi catchment to diminish

6.2 Limitations and future scope of work

- Due to geospatial limitation, numerous uncertainty and vulnerability exist in the hydrological impacts scenarios in climate modeling. However, also climate signal transformation to meteorological stations for hydrological representation still with ambiguity. The model simulation has not considered land use changes unequivocally in spite of the fact that overall considered, in land use may associate with climate prompting diverse projections for future hydrological conditions. Hence, the consequences of this examination ought to be taken with consideration and be considered as a sign of likely future changes as opposed to a realistic expectation.

- The GCMs were downscaled to catchment scale utilizing the Statistical down-Scaling Model (SDSM) which is a regression-based model. There additionally other downscaling models, which are normally connected in climate change, impact evaluation. Nevertheless, it isn't yet clear which techniques give the most solid gauge for future climate. Truth be told, all downscaling techniques are still particularly improvement and testing stage Xu et al, (2005). Therefore, other downscaling models ought to likewise be tried to permit an appraisal of the outcome from the distinctive downscaling model.

- Water resources are inseparably connected with the climate, so the possibility of worldwide climate change has genuine ramifications for water assets. As water resources, stresses wind up intense later on as the consequence of a mix of climate impacts and raising human interest, there will heighten clashes among human and ecological demand on water resources. Hence, there is a need to limit the affectability to environmental change. One approach to limit chance is to make the economy progressively expanded, and rural innovation ought to improve water use through the production of the water system and harvest advancement. Also, inquire about exercises ought to be strengthened around there to investigate the effect of climate change on different parts including water assets by incorporating with recent findings.

REFERENCES

A. Bronstert, V. K., 1999. Modelling river discharge for large drainage basins: from lumped to distributed approach. *Hydrological Sciences,* 44(2), pp. 313-331.

A. E. Majule, A. L. M., 2009. Impacts of climate change, variability and adaptation strategies on agriculture in semi-arid areas of Tanzania. *African Journal of Environmental Science and Technology,* 3(8), pp. 206-218.

A. G. Koutroulis, M. G. G. I. K. T., 2010. Application of the HBV hydrological model in a flash flood. *Natural Hazards and Earth System Science,* Issue 10, pp. 2713-2724.

Arne Forsman, S. B., 1973. Development of a Conceptual Deterministic Rainfall-Runoff Model. *Nordic Hydrology,* Issue 4, pp. 147-170.

Asfaw Kebede, E. A., 2017. Assessment of Climate Change Impacts on the Water Resources of Megech River Catchment, Abbay Basin, Ethiopia. *Open Journal of Modern Hydrology,* Issue 7, pp. 141-152.

Assefa M. Melesse, S. B. D., 2012. Impact and uncertainties of climate change on the hydrology of the Mara River basin, Kenya/Tanzania. *Hydrological Processes,* 10(27), pp. 2973-2986.

Axel Ritter, R. M.-C., 2013. Performance Evaluation of Hydrological Model: Statistical significance for reducing subjectivity in the goodness of fit assessment. *Journal oF Hydrology,* Volume 480, pp. 33-45.

Barbro Johansson, G. B. J. G. H. G. H., 2009. *Improvement HBV model Rhine in FEWS,* Norrköping: Swedish Meteorological and Hydrological Institute.

Ben Kirtman, 2019. *Dynamic Downscaling: Issues and Considerations.* [Online] Available at: http://www.ces.fau.edu/climate_change/downscaling/pdfs/kirtman-ppt.pdf [Accessed 1 March 2019].

Booij, M. J., 2004. Impact of climate change on river flooding assessed with different spatial model resolutions. *Journal of Hydrology,* 303(7), pp. 177-198.

Booij, M. J., 2004. Impact of climate change on river flooding assessed with different spatial model resolutions. *Journal of Hydrology,* Issue 303, pp. 177-198.

Chad Shouquan Cheng, Q. L. G. L., 2011. A Synoptic Weather-Typing Approach to Project Future Daily Rainfall and Extremes at Local Scale in Ontario, Canada. *Journal of Climate,* Volume 24, pp. 3667-3685.

Chong-yu Xu, C.-y. X. E. W. S. H., 2005. Modelling Hydrological Consequences of Climate Change. *Advances in Atmospheric Sciences,* 22(6), p. 789–797.

Christian Leibundgut & Allan Rodhe, S. U. J. S., 2009. Prediction uncertainty of conceptual rainfall-runoff models caused by problems in identifying model parameters and structure. *Hydrological Sciences Journal*, 34(10), pp. 779-795.

Christian Leibundgut & Allan Rodhe, S. U. J. S., 2009. Prediction uncertainty of conceptual rainfall-runoff models caused by problems in identifying model parameters and structure. *Hydrological Sciences Journal*, Issue 10, pp. 779-795.

Daniel S. Wilks, 2019. *Wiley.* [Online] Available at: https://onlinelibrary.wiley.com/doi/epdf/10.1002/wcc.85 [Accessed 1 March 2019].

E. Todini, 2007. Hydrological catchment modeling: past, present, and future. *Hydrology & Earth System Science,* 11(1), pp. 468-482.

Energy, D. o. E. a., 2019. *Australian Government.* [Online] Available at: http://www.environment.gov.au/system/files/resources/492978e6-d26b-4202-ae51-5eba10c0b51a/files/wa-rcp-fact-sheet.pdf [Accessed 28 February 2019].

H. A. Pahlavan, A. M. V. B. Z., 2018. Improvement of multiple linear regression method for statistical downscaling of monthly precipitation. *International Journal of Environmental Science Technology,* Volume 25, p. 1897–1912.

Hardy, J. T., 2003. *Climate Change Causes, Effects, and Solutions.* 1st ed. Washington: Wiley.

Hunukumbura, 2008. The potential to narrow uncertainties in regional precipitation change. *Journal of climate dynamics,* 37(6), pp. 407-418.

IPCC, 2007. *Impacts, Adaptation and Vulnerability,* Geneva: WMO.

IPCC, 2013. *IPCC Fifth Assessment Report,* Geneva: European Climate Foundation.

J. Merz, S. N. M. K., 2010. An application of the HBV model to the Tamor Basin in Eastern Nepal. *Journal of Hydrology and Meteorology,* 7(1), pp. 49-58.

J. Seibert, M. J. P. V., 2012. Teaching hydrological modeling with a user-friendly catchment-runoff-model software package. *Hydrology and Earth System Sciences,* Issue 16, p. 3315–3325.

J.J. Kashaigili, A. M., 2010. Integrated assessment of land use and cover changes in the Malagarasi river catchment in Tanzania. *Physics and Chemistry of the Earth,* Issue 35, pp. 730-741.

Jan Seibert, S. U. C. L., 2005. Prediction uncertainty of conceptual rainfall-runoff models caused by problems to identify model parameters and structure. *Hydrological Sciences,* 44(5), p. 779–798.

Jones, R., 2017. *Uncertainty in climate change impacts on Southern Alps river flows the role of hydrological model complexity,* Dunedin: University of Otago.

Julie K. H. Zimmerman, N. L. P., 2010. Ecological responses to altered flow regimes: a literature review to inform the science and management of environmental flows. *Freshwater Biology,* Issue 55, pp. 194-205.

K. J. Beven, J. S., 2009. Gauging the ungauged basin: how many discharge measurements?. *Hydrology and Earth System Sciences,* Issue 13, p. 883–892.

Kendal McGuffie, A. H., 2005. A Climate Modelling Primer. In: K. McGuffie, ed. *A Climate Modelling Primer*. Sydney: John Wiley and Sons Ltd, pp. 7-9.

Linda O. Mearns, 2009. *National Center for Atmospheric Research.* [Online] Available at: https://www.narccap.ucar.edu/users/user-meeting-09/talks/Downscaling_summary_for_NARCCAP_Users_Meet09.pdf
[Accessed 2 March 2019].

Marie Gardelin, G. L. B. J., 1997. Development and Test of the Distributed HBV-96 Hydrological Model. *Journal of Hydrology,* Volume 201, pp. 272-288.

N. A. M. Arish, N. A. M. R. J. A., 2010. Flood Estimation Studies using Hydrologic Modeling System (HEC-HMS) for Johor River, Malaysia. *Journal of Applied Science,* 10(11), pp. 930-939.

P. Krause, . F. B. D. P. B., 2005. Comparison of different efficiency criteria for hydrological model assessment. *Advances in Geosciences,* Volume 5, p. 89–97.

P. Nolan, S. W. R. M., 2006. The impact of climate change on the discharge of Suir River Catchment (Ireland) under different climate scenarios. *Natural Hazards and Earth System Sciences,* 23(6), pp. 387-394.

Priyantha Ranjan Sarukkalige, H. I. J. A.-S., 2017. Assessment of future climate change impacts on hydrological behavior of Richmond River Catchment. *Water Science and Engineering,* 10(3), pp. 197-208.

R. Uijlenhoet, T. L. A. D. R. T. W. L. H., 2010. The hydrological response of the Ourthe catchment to climate change as modeled by the HBV model. *Hydrology and Earth System Science,* Issue 14, pp. 651-665.

Roy Gu, M. J. Z. P. E. S. T., 2003. The Impacts of Climate Change on Stream Flow in the Upper Mississippi River Basin: A Regional Climate Model Perspective. *Journal of Hydrol Science,* 337(03), pp. 1-26.

Rozeana Hj Md. Juani, S. S., 2015. Flow Assessment of Brunei River due to the Impact of Climate Change. *4th International Conference on Environmental, Energy, and Biotechnology,* 85(5), pp. 28-34.

Safar Marofi, R. S. M. M. A., 2018. A Multi-GCM Assessment of the Climate Change Impact on Hydrology and Hydropower Potential of a Semi-Arid Basin. *Water,* Issue 10, pp. 5-17.

S

APPENDIX

A: Rainfall

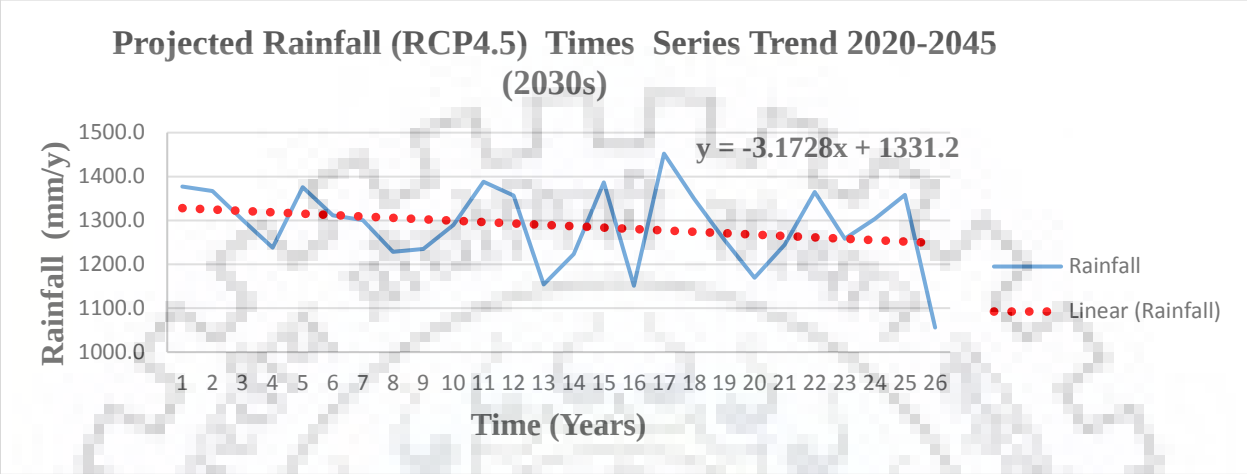

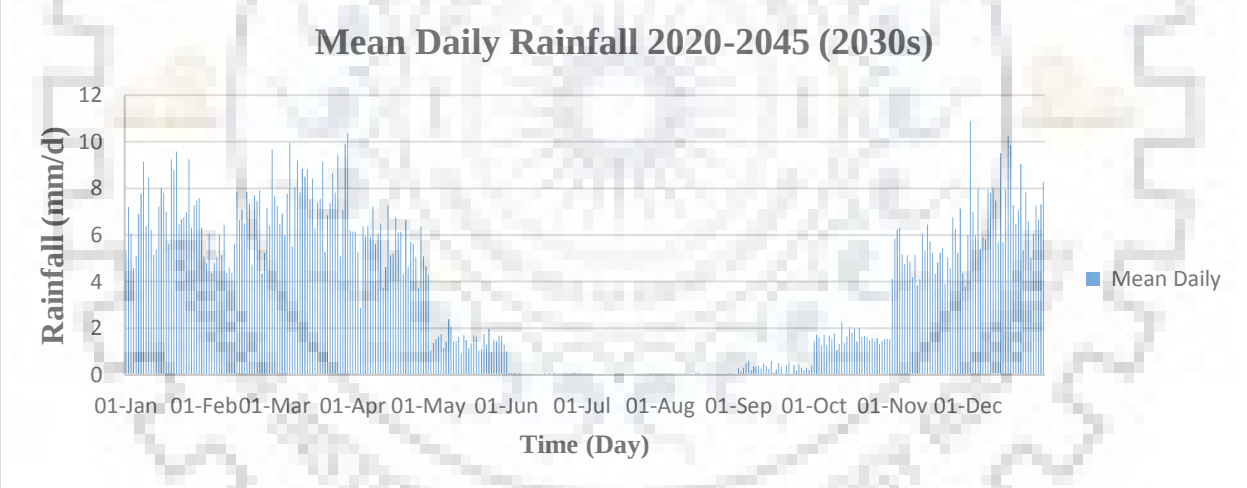

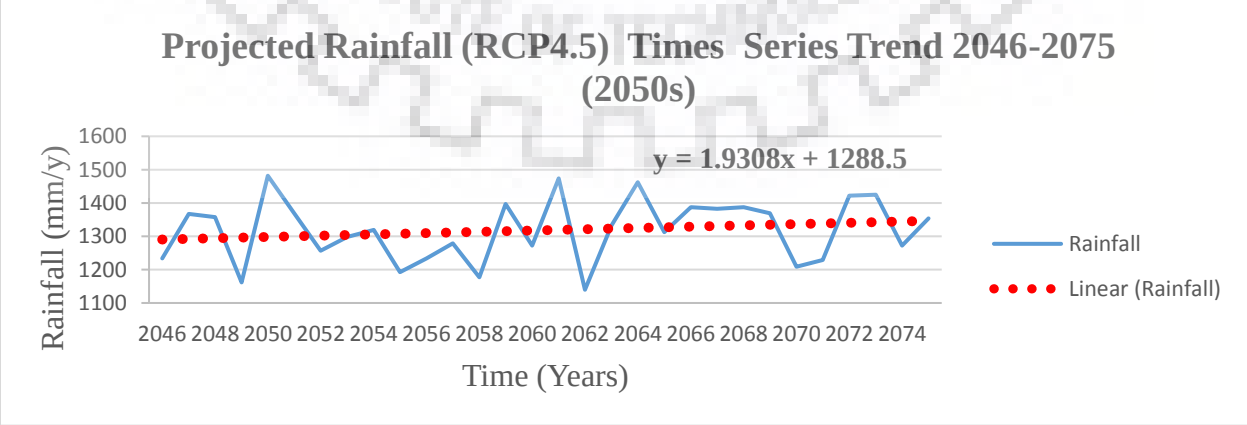

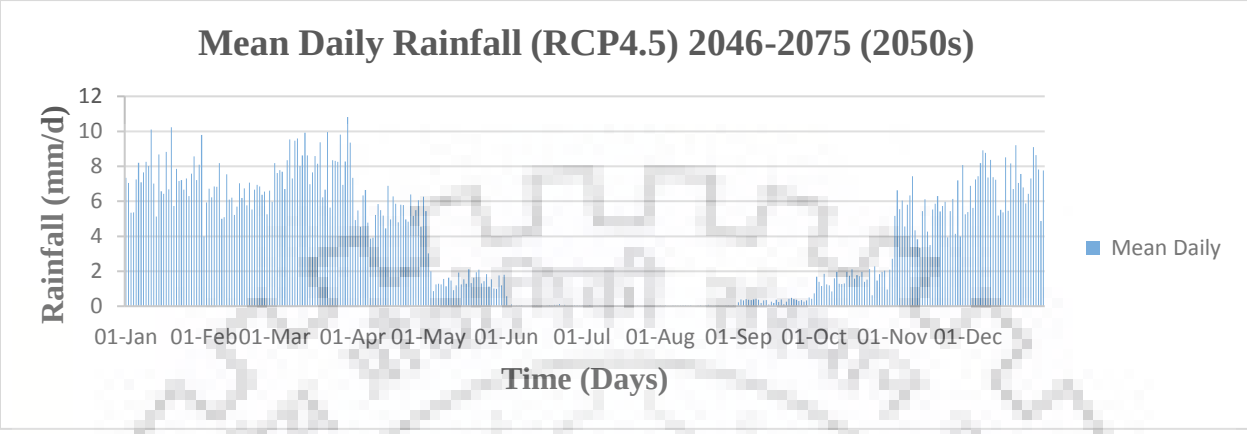

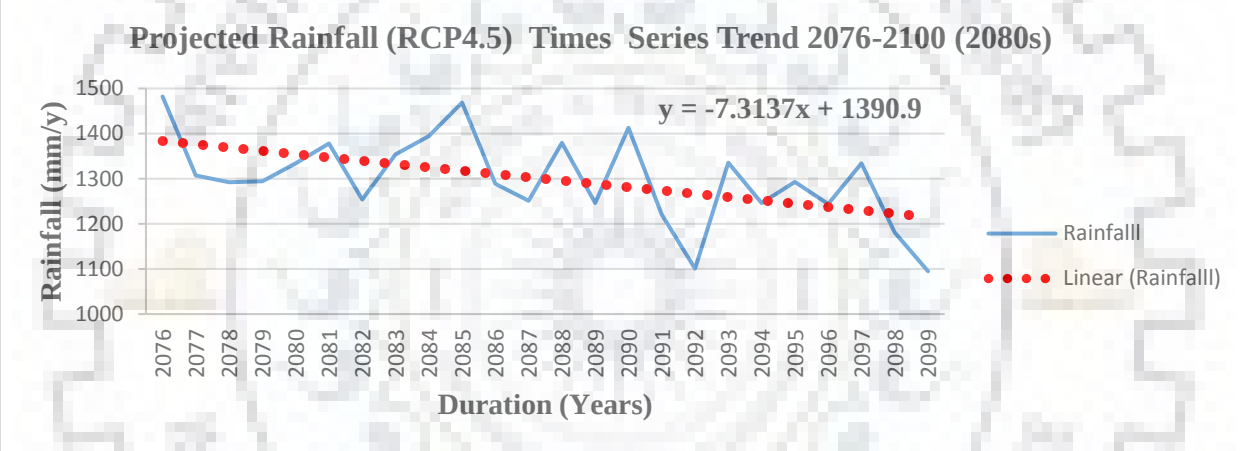

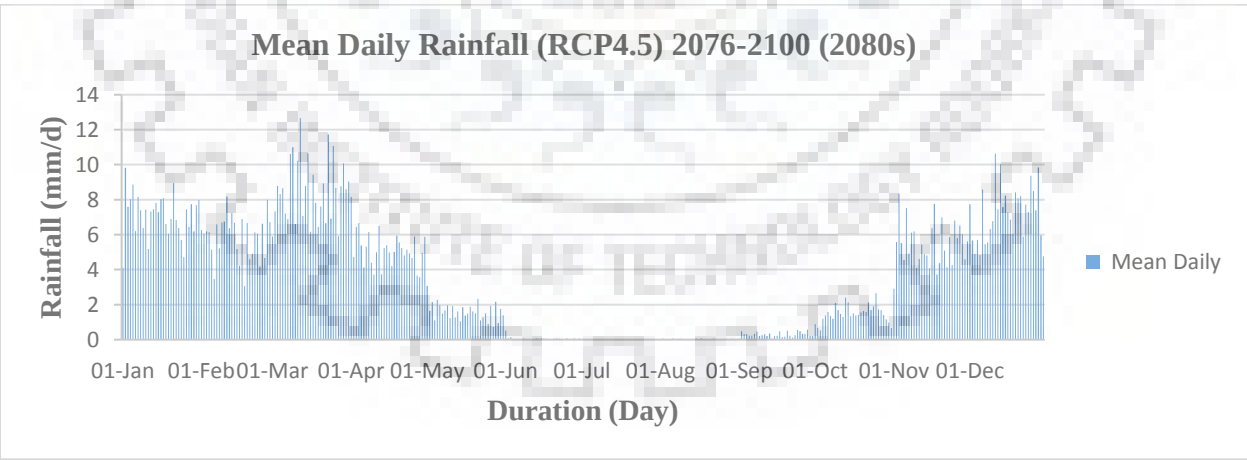

B: Temperature

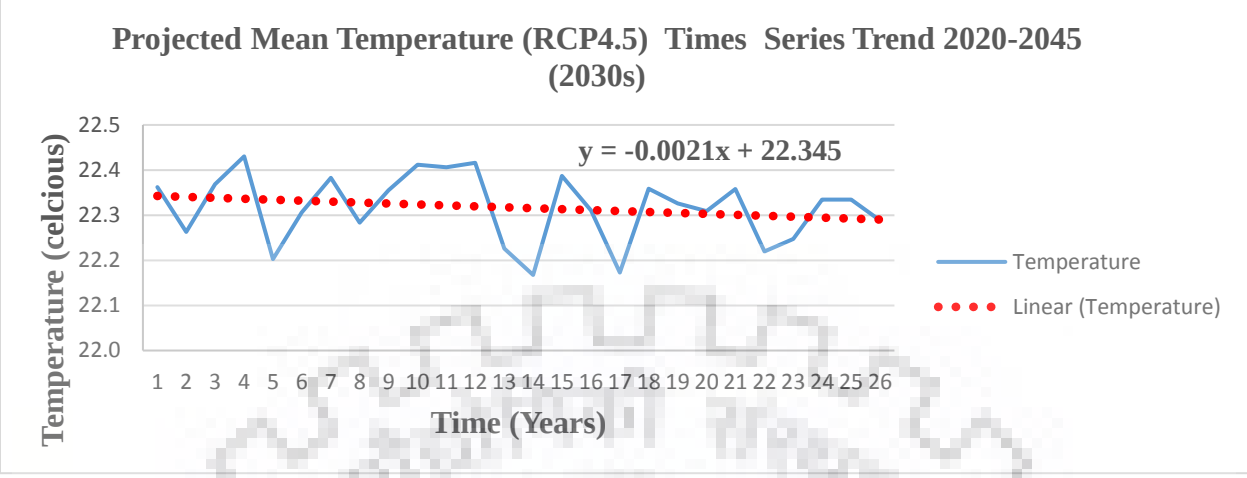
Projected Mean Temperature (RCP4.5) Times Series Trend 2020-2045 (2030s)
y = -0.0021x + 22.345
Temperature (celcious)
Time (Years)
Temperature
Linear (Temperature)

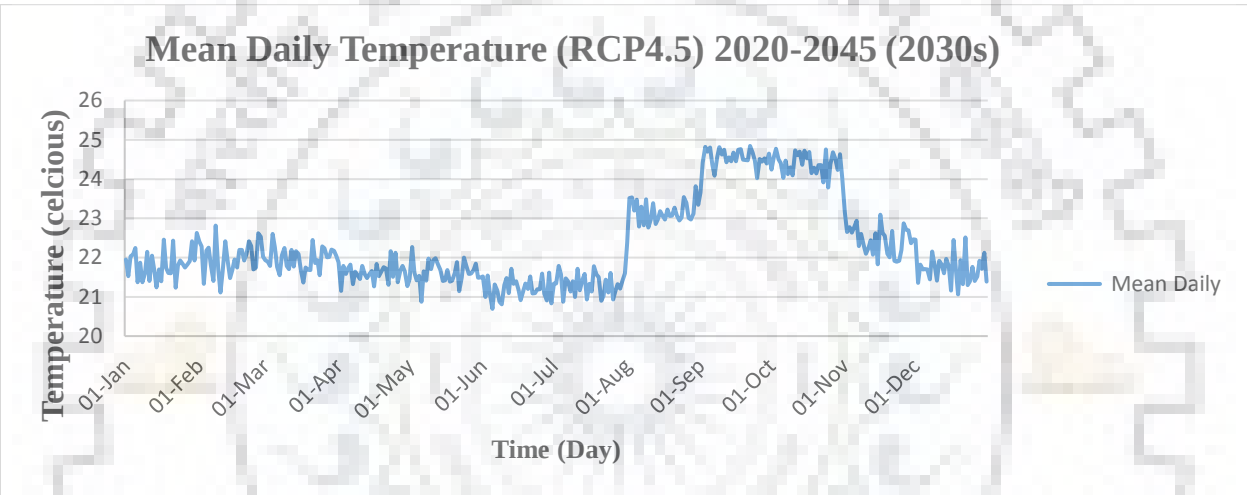
Mean Daily Temperature (RCP4.5) 2020-2045 (2030s)
Temperature (celcious)
Time (Day)
Mean Daily

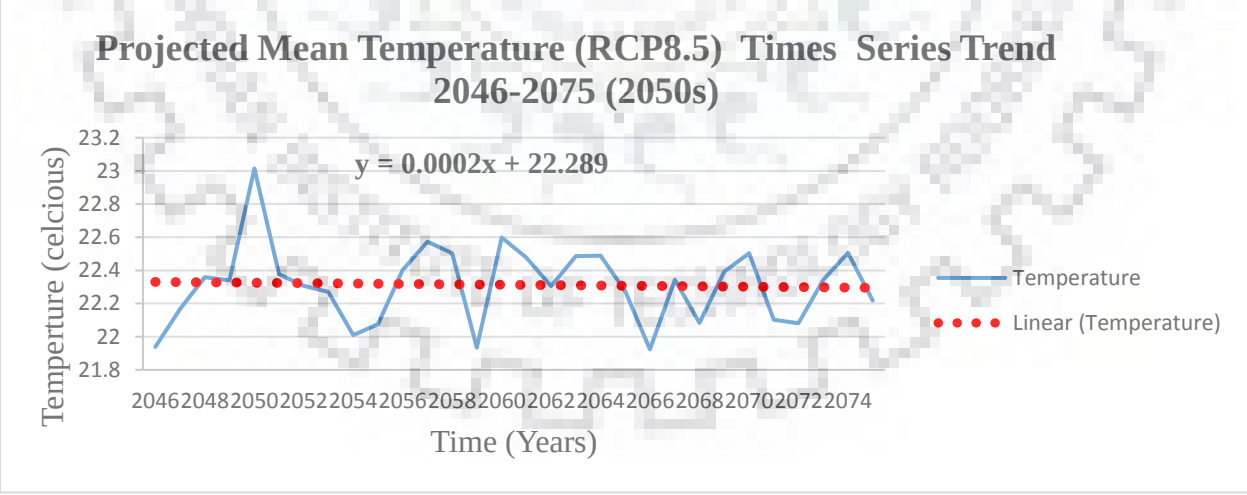
Projected Mean Temperature (RCP8.5) Times Series Trend 2046-2075 (2050s)
y = 0.0002x + 22.289
Temperture (celcious)
Time (Years)
Temperature
Linear (Temperature)

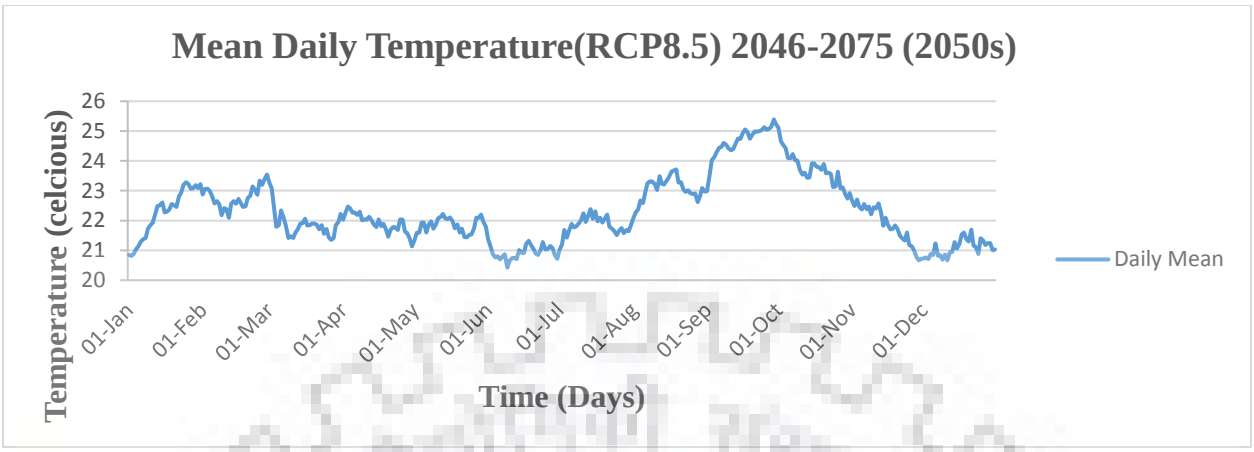
Mean Daily Temperature(RCP8.5) 2046-2075 (2050s)
Temperature (celcious)
26
25
24
23
22
21
20
01-Jan
01-Feb
01-Mar
01-Apr
01-May
01-Jun
01-Jul
01-Aug
01-Sep
01-Oct
01-Nov
01-Dec
Time (Days)
Daily Mean

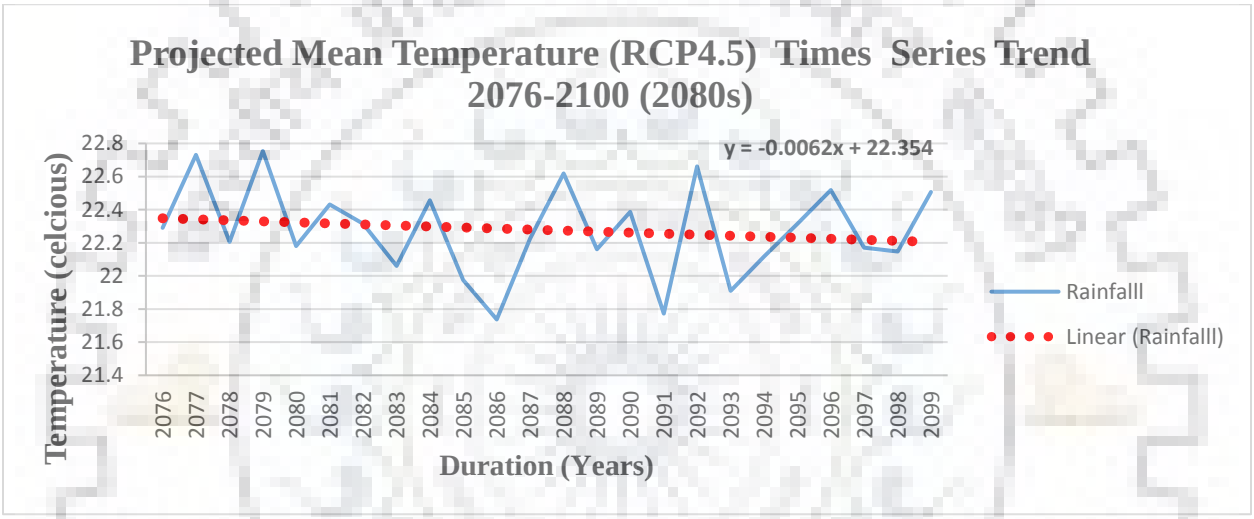
Projected Mean Temperature (RCP4.5) Times Series Trend 2076-2100 (2080s)
y = -0.0062x + 22.354
Temperature (celcious)
22.8
22.6
22.4
22.2
22
21.8
21.6
21.4
2076
2077
2078
2079
2080
2081
2082
2083
2084
2085
2086
2087
2088
2089
2090
2091
2092
2093
2094
2095
2096
2097
2098
2099
Duration (Years)
Rainfalll
Linear (Rainfalll)

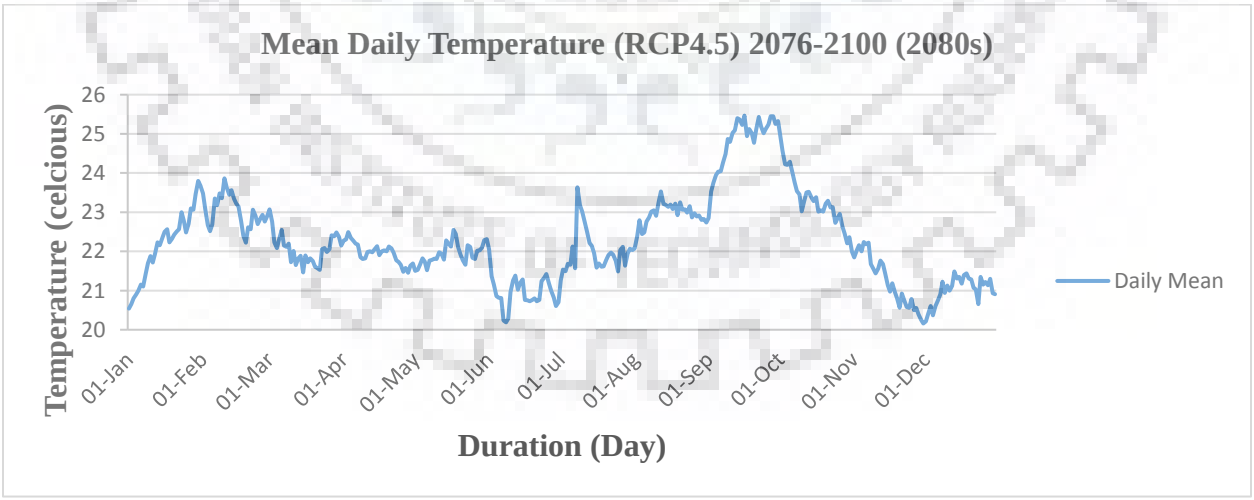
Mean Daily Temperature (RCP4.5) 2076-2100 (2080s)
Temperature (celcious)
26
25
24
23
22
21
20
01-Jan
01-Feb
01-Mar
01-Apr
01-May
01-Jun
01-Jul
01-Aug
01-Sep
01-Oct
01-Nov
01-Dec
Duration (Day)
Daily Mean

C: SDSM Results for Rainfall

RESULTS: EXPLAINED VARIANCE

Analysis Period: 01/01/1979 - 31/12/2012
Significance level: 0.05

Total missing values: 0

Predictand: Observed_Rainfall12.DAT

Predictors:	JAN	FEB	MAR	APR	MAY	JUN	JUL	AUG	SEP	OCT	NOV	DEC
h3a2p_uaf.DAT		0.010										
h3a2rhumaf.DAT					0.009		0.005			0.008		
h3a2shumaf.DAT			0.009						0.008		0.015	
h3a2tempaf.DAT									0.005	0.006	0.019	

CORRELATION MATRIX

Analysis Period: 01/01/1979 - 31/12/2012 (Annual)

Missing values: 0
Missing rows: 0
Values less than or equal to threshold: 3165

		1	2	3	4	5
1	Observed_Rainfall12.DAT	1	0.053	-0.076	0.240	0.273
2	h3a2p_uaf.DAT	0.053	1	0.040	0.372	0.283
3	h3a2rhumaf.DAT	-0.076	0.040	1	-0.113	-0.218
4	h3a2shumaf.DAT	0.240	0.372	-0.113	1	0.933
5	h3a2tempaf.DAT	0.273	0.283	-0.218	0.933	1

PARTIAL CORRELATIONS WITH Observed_Rainfall12.DAT

	Partial r	P value
h3a2p_uaf.DAT	-0.013	0.2513
h3a2rhumaf.DAT	-0.006	0.4860
h3a2shumaf.DAT	-0.035	0.0022
h3a2tempaf.DAT	0.128	0.0000

D: Scatter plots of observed rainfall and GCM predictors

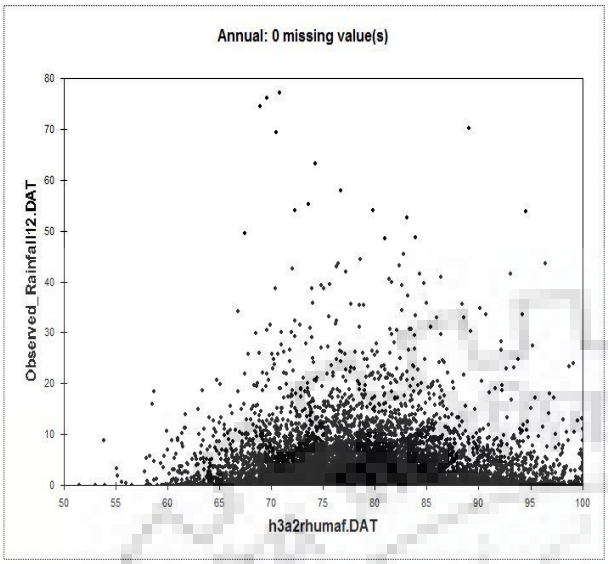
Annual: 0 missing value(s)
Observed_Rainfall12.DAT
h3a2rhumaf.DAT

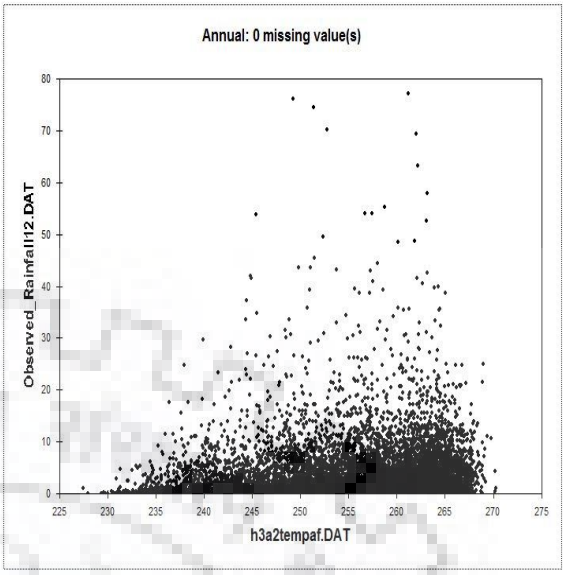
Annual: 0 missing value(s)
Observed_Rainfall12.DAT
h3a2tempaf.DAT

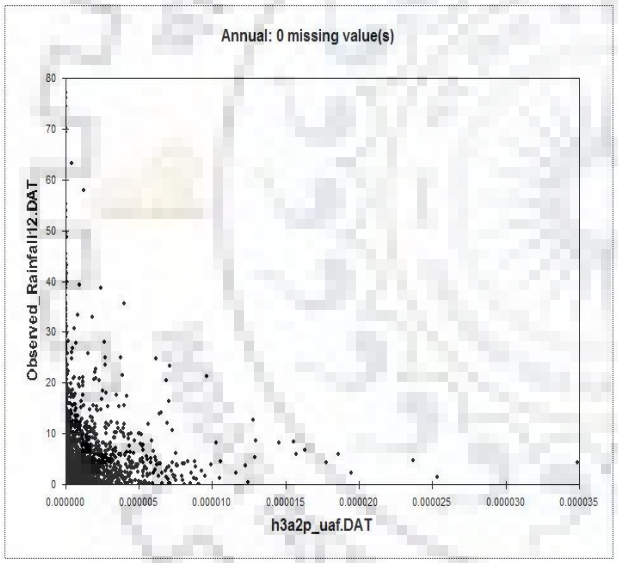
Annual: 0 missing value(s)
Observed_Rainfall12.DAT
h3a2p_uaf.DAT

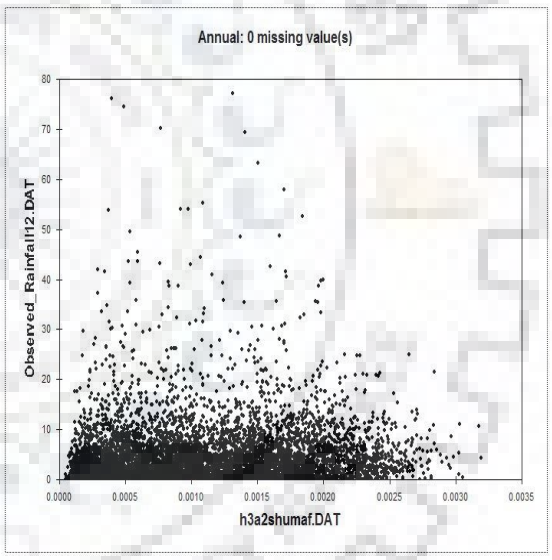
Annual: 0 missing value(s)
Observed_Rainfall12.DAT
h3a2shumaf.DAT

Predictand: Observed_Rainfall12.DAT

Predictors:
h3a2p_uaf.DAT
h3a2rhumaf.DAT
h3a2shumaf.DAT
h3a2tempaf.DAT

Unconditional Statistics

Month	RSquared	SE	Chow	Durbin-Watson
January	0.001	5.838	2.5949	1.307
February	0.000	5.999	0.7594	1.281
March	0.004	7.874	0.7553	1.347
April	0.008	5.154	3.4355	1.165
May	0.001	1.986	2.1581	1.067
June	0.000	0.186	0.9704	1.653
July	0.001	0.079	-5.3388	1.494
August	0.000	0.157	0.4491	1.389
September	0.005	0.772	0.2031	1.676
October	0.015	2.504	0.5600	1.241
November	0.010	6.334	4.2316	1.204
December	0.000	6.291	3.4969	1.214
Mean	0.004	3.598	1.1896	1.336

Month	Mean	Maximum	Minimum	Median	Variance	Sum	ACF
January	5.694	20.989	0.000	4.946	25.182	176.506	-0.001
February	5.920	21.338	0.000	5.361	25.116	166.931	-0.011
March	7.218	28.059	0.000	6.248	41.677	223.773	-0.022
April	4.738	17.466	0.000	4.003	18.697	142.137	0.025
May	1.311	6.513	0.000	0.867	2.124	40.634	-0.006
June	0.064	0.470	0.000	0.001	0.010	1.917	-0.016
July	0.079	0.297	0.000	0.071	0.005	2.456	0.024
August	0.151	0.560	0.000	0.134	0.017	4.676	-0.021
September	0.348	2.037	0.000	0.070	0.228	10.435	-0.006
October	1.487	7.337	0.000	0.830	3.055	46.091	0.046
November	5.051	21.614	0.000	3.968	25.870	151.535	-0.024
December	6.145	21.544	0.000	5.509	26.809	190.489	-0.003
Winter	5.919	23.256	0.000	5.291	25.841	444.939	-0.001
Spring	4.419	28.059	0.000	2.473	26.879	406.543	0.214
Summer	0.098	0.567	0.000	0.067	0.012	9.050	0.106
Autumn	2.286	21.614	0.000	0.560	13.676	208.061	0.277
Annual	3.170	28.136	0.000	0.496	21.420	1157.580	0.341
Standard Deviations of Results							
January	0.375	1.780	0.000	0.562	2.968	11.634	0.098
February	0.282	2.872	0.000	0.455	2.752	7.965	0.076
March	0.618	2.358	0.000	0.646	5.974	19.151	0.072
April	0.290	1.829	0.000	0.435	2.340	8.711	0.064
May	0.110	0.826	0.000	0.195	0.239	3.401	0.082
June	0.008	0.067	0.000	0.003	0.002	0.246	0.073
July	0.004	0.034	0.000	0.005	0.001	0.115	0.085
August	0.010	0.049	0.000	0.016	0.002	0.325	0.067
September	0.044	0.289	0.000	0.083	0.043	1.308	0.076
October	0.106	0.882	0.000	0.241	0.415	3.285	0.105
November	0.504	2.486	0.000	0.809	3.314	15.115	0.076
December	0.355	1.956	0.000	0.515	2.582	11.012	0.082
Winter	0.177	2.023	0.000	0.255	1.285	13.307	0.057
Spring	0.256	2.358	0.000	0.216	3.493	23.597	0.053
Summer	0.005	0.046	0.000	0.007	0.001	0.461	0.038
Autumn	0.183	2.486	0.000	0.116	1.818	16.687	0.054
Annual	0.089	2.320	0.000	0.076	0.929	32.575	0.035

E: SDSM Results for Temperature

RESULTS: EXPLAINED VARIANCE

Analysis Period: 01/01/1979 - 31/12/2012
Significance level: 0.05

Total missing values: 0

Predictand: Observed_Temp.DAT

Predictors:	JAN	FEB	MAR	APR	MAY	JUN	JUL	AUG	SEP	OCT	NOV	DEC
h3a2p_uaf.DAT												
h3a2rhumaf.DAT			0.011		0.008			0.022				
h3a2shumaf.DAT	0.006			0.013		0.007			0.005	0.007	0.018	
h3a2tempaf.DAT	0.006	0.007	0.006	0.011		0.007			0.006	0.011	0.030	

CORRELATION MATRIX

Analysis Period: 01/01/1979 - 31/12/2012 (Annual)

Missing values: 0
Missing rows: 0

		1	2	3	4	5
1	Observed_Temp.DAT	1	-0.056	0.034	-0.135	-0.089
2	h3a2p_uaf.DAT	-0.056	1	0.033	0.375	0.287
3	h3a2rhumaf.DAT	0.034	0.033	1	-0.086	-0.161
4	h3a2shumaf.DAT	-0.135	0.375	-0.086	1	0.932
5	h3a2tempaf.DAT	-0.089	0.287	-0.161	0.932	1

PARTIAL CORRELATIONS WITH Observed_Temp.DAT

	Partial r	P value
h3a2p_uaf.DAT	0.012	0.2228
h3a2rhumaf.DAT	0.047	0.0000
h3a2shumaf.DAT	-0.147	0.0000
h3a2tempaf.DAT	0.111	0.0000

F: Scatter plot observed temperature and GCM predictors

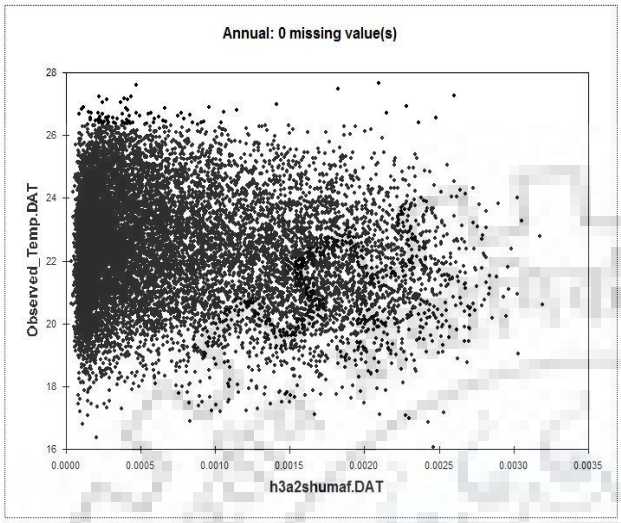

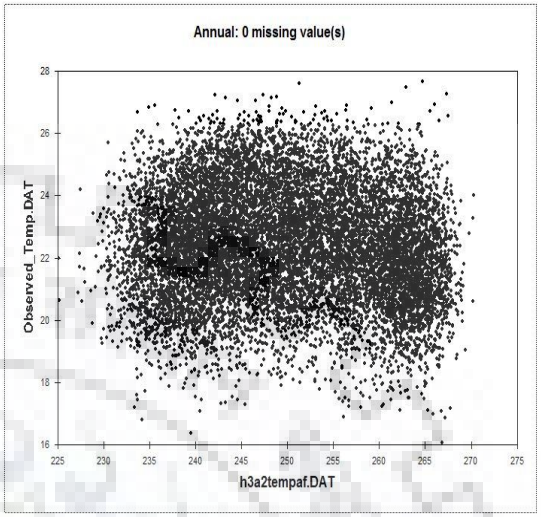

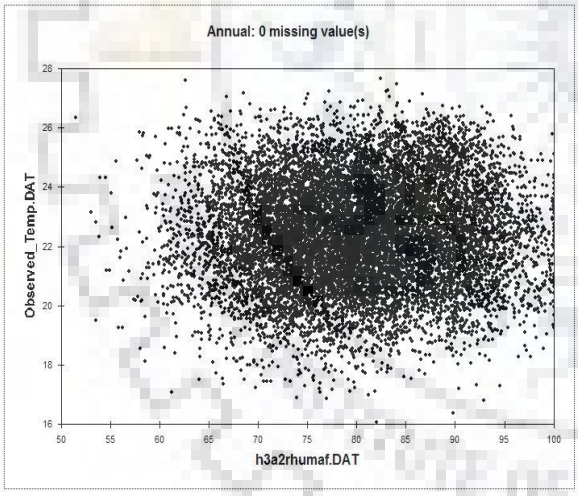

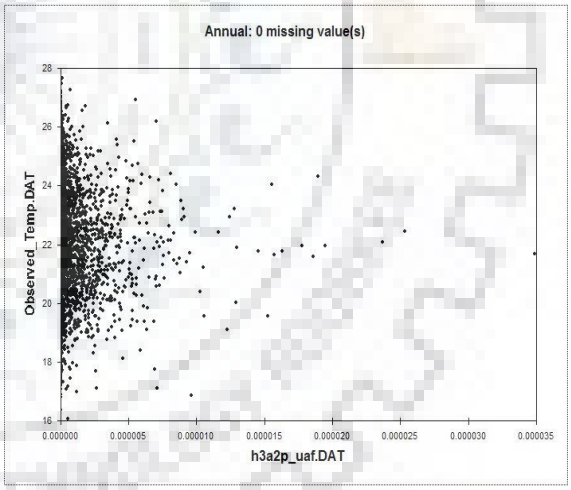

Predictand: Observed_Temp.DAT

Predictors:
h3a2p_uaf.DAT
h3a2rhumaf.DAT
h3a2shumaf.DAT
h3a2tempaf.DAT

Unconditional Statistics

Month	RSquared	SE	Chow	Durbin-Watson
January	0.006	1.575	24.9544	0.547
February	0.007	1.657	10.2187	0.602
March	0.009	1.631	5.4188	0.501
April	0.025	1.319	36.0208	0.492
May	0.034	1.368	21.6230	0.551
June	0.006	1.348	10.8595	0.626
July	0.008	1.322	2.3050	0.706
August	0.032	1.258	3.5112	0.691
September	0.013	1.019	2.4868	0.837
October	0.007	1.119	- 0.3185	0.813
November	0.042	1.544	5.1810	0.508
December	0.001	1.643	18.6307	0.587
Mean	0.016	1.400	11.7410	0.622

Month	Mean	Maximum	Minimum	Median	Variance	Sum	ACF	Skewnes
January	21.916	25.845	17.680	21.883	2.451	679.392	0.028	-0.018
February	22.119	26.436	17.752	22.131	2.830	623.748	0.021	0.022
March	21.838	26.481	17.338	21.806	2.825	676.971	-0.008	0.047
April	21.671	25.112	18.288	21.683	1.805	650.144	0.025	-0.024
May	21.653	25.543	17.824	21.684	1.926	671.255	0.027	-0.014
June	21.052	24.631	17.536	21.029	1.891	631.557	-0.022	0.031
July	21.320	25.067	17.950	21.299	1.673	660.914	-0.048	0.134
August	22.872	26.331	19.473	22.887	1.653	709.028	0.068	-0.055
September	24.448	27.226	21.888	24.434	1.056	733.437	0.023	0.093
October	24.334	27.184	21.328	24.355	1.251	754.347	-0.024	-0.091
November	22.800	26.813	18.533	22.774	2.498	684.007	0.044	-0.038
December	21.655	25.969	17.247	21.685	2.680	671.319	0.006	-0.031
Winter	21.890	26.599	16.942	21.890	2.699	1645.383	0.035	-0.002
Spring	21.721	26.588	17.119	21.716	2.202	1998.370	0.016	0.050
Summer	21.755	26.343	17.314	21.728	2.390	2001.499	0.265	0.065
Autumn	23.866	27.470	18.533	24.035	2.164	2171.791	0.273	-0.562
Annual	22.306	27.577	16.606	22.264	3.177	8146.119	0.363	0.038
Standard Deviations of Results								
January	0.115	0.433	0.741	0.163	0.208	3.561	0.081	0.135
February	0.139	0.533	0.696	0.199	0.380	3.912	0.091	0.199
March	0.121	0.783	0.526	0.157	0.407	3.766	0.072	0.139
April	0.084	0.581	0.452	0.109	0.254	2.511	0.090	0.140
May	0.074	0.371	0.630	0.097	0.140	2.302	0.082	0.192
June	0.100	0.564	0.584	0.126	0.197	2.993	0.072	0.181
July	0.116	0.488	0.616	0.153	0.164	3.596	0.075	0.213
August	0.081	0.585	0.467	0.113	0.154	2.506	0.073	0.211
September	0.069	0.309	0.297	0.078	0.127	2.056	0.075	0.172
October	0.095	0.317	0.436	0.102	0.120	2.948	0.089	0.171
November	0.123	0.522	0.605	0.130	0.259	3.678	0.081	0.171
December	0.171	0.674	0.475	0.226	0.251	5.290	0.090	0.184
Winter	0.072	0.500	0.525	0.107	0.188	5.408	0.051	0.086
Spring	0.061	0.693	0.514	0.066	0.197	5.622	0.042	0.110
Summer	0.051	0.573	0.562	0.071	0.139	4.707	0.036	0.099
Autumn	0.063	0.325	0.605	0.076	0.159	5.705	0.049	0.115
Annual	0.033	0.302	0.464	0.042	0.079	12.211	0.020	0.039